ENGINEERING EXPERIMENT STATION
of the Georgia Institute of Technology
Atlanta, Georgia

FINAL REPORT

PROJECT NO. B-229

CENTRIFUGAL SEPARATION AND CLASSIFICATION

by

JOHN H. BURSON, KOICHI IINOYA, and CLYDE ORR

COVERING THE PERIOD
JANUARY 1, 1961 through DECEMBER 31, 1962

RESEARCH GRANT NO. AP-127 (C1)

Prepared for

DIVISION OF AIR POLLUTION
BUREAU OF STATE SERVICES
DEPARTMENT OF HEALTH, EDUCATION, AND WELFARE
WASHINGTON 25, D. C.

TABLE OF CONTENTS

This report contains 55 pages.

LIST OF FIGURES

LIST OF FIGURES (Continued)

LIST OF TABLES

I. SUMMARY

The purpose of this study was to investigate further the use of centrifugal force as a means of removing suspended particulate matter down to sub-micron size from an airstream. Theoretical studies were made of many of the limiting design and collection factors and a rotary centrifugal separator was constructed and evaluated by means of a number of aerosols of widely differing properties. The device was shown to remove particulate matter from an air stream at moderate rotation speeds, i.e., up to 6000 rpm, with efficiencies of nearly 100 per cent. The collection efficiency on a mass basis showed a linear relationship with the square root of the volumetric flow rate divided by the rotational speed when plotted on a logarithmic-probability graph. This experimental relationship was justified by a rather simple theory which combines the assumed particle cut diameter of the separator with a logarithmic normal distribution of particle sizes. The linear relation did not hold above about 6000 rpm and was believed to be due to a transition from laminar to turbulent flow within the rotor. The present design for a centrifugal separator has provision for the periodic introduction of water counter to the normal flow of clean air, thus washing down the material collected on the rotor and thereby permitting essentially continuous operation.

A special design of centrifugal separator rotor was constructed and evaluated after it was observed that the material collected on the separator rotor was fairly well classified according to size. Provision was made to introduce a secondary stream of particle-free air counter to the trajectories of the aerosol particles. The presence of this additional

drag force enabled the deposition of particles to be spread over a wider area, thus effecting a more efficient classification. Promising results were obtained in the classification of aerosols of irregular particles such as talc and of regular particles such as glass beads. The resulting classification was strongly dependent on the extent of particle deagglomeration and the dispersion achieved and upon such operating variables as rotor speed, aerosol flow rate, pressure rise and secondary air flow rate.

Further studies should be made to determine what design changes are necessary to stabilize the flow within the centrifugal separator at high flow rates and rotor speeds without excessively increasing the overall pressure drop. The elimination of the transition from laminar to turbulent flow and the decrease of friction losses in the bearing system may enable the centrifugal separator to compete economically with more convential devices such as filters or cyclones. Further testing of the centrifugal classifier is also desirable to determine the quantitative effects of many of the operating variables. If possible, the type of flow field present in the classifier rotor should be determined, i.e., it should be established whether the field is a forced vortex, free vortex, etc., and the resulting classification should be compared with that theoretically predicted from a claculation of particle trajectories in the same types of force field.

II. INTRODUCTION

The development of new branches of industry and the appearance of new technological processes requiring atmospheres essentially free of suspended particulate matter have created a great need for new types of equipment to provide highly purified air. Thus the initial purpose of this study was to investigate the use of a centrifugal device for removing particulate matter down to sub-micron diameters from an air stream. It was believed that by proper design many of the desirable features of inertial separation devices could be combined with the high separation efficiencies attainable with disk-type centrifuges. In principle, a device operating on the above criteria is more efficient than most filtering devices, is more compact, has more predictable operating characteristics and is capable of essentially continuous operation.

In order to extract particulate matter down to sub-micron diameters from an air stream with efficiences approaching 100 per cent, the device must operate at the highest rotation speeds attainable from the standpoint of strength of rotor material. It is also necessary, for high separation efficiencies, to maintain laminar flow throughout the system. This, in turn, requires the use of converging conduits to stabilize the accelerating flow which, of necessity, also creates undesirable high pressure drops through the system. Thus some design compromises are necessary to achieve optimum overall operation. To operate continuously, provision must be made for the periodic injection of water or some other fluid to wash down the accumulated material on the rotor. Also it is desirable to design the system so that the natural pumping action of the rotor will provide a

sufficient gas flow rate so that no external blower will be required to operate the unit.

It was discovered during the course of experiments on particle separation that the material collected on the rotor was fairly well classified according to size. Consequently, additional theoretical and experimental studies were undertaken to predict the resulting classification and a special rotor was designed to classify as well as to separate.

III. THEORETICAL STUDIES

The design of centrifugal separators and classifiers, their operating requirements and the interpretation of data therefrom are far from straightforward. Therefore, the following theoretical studies were undertaken to provide information on design limitations, particle and fluid mechanics in various types of centrifugal fields and various other operating characteristics.

A. Design Considerations

1. Calculation of Required Rotor Strength

Hoop tension, σ, which relates required rotor material strength to the centrifugal force available, is given by equation 1 in which ρ_m is the density of the rotor material, r_3 is the radius of rotation, ω is the angular velocity, N is the rotor speed, and g_c is the force-mass conversion factor.

$$\sigma = \frac{\rho_m \, r_3^2 \, \omega^2}{g_c} = \frac{4\pi^2 \, \rho_m \, N^2 \, r_3^2}{g_c} \qquad (1)$$

As a typical example, the hoop tension was calculated for a rotor radius of 12.5 cm, a density of 3 gm/cm^3 (as would be the case for aluminum) and a rotor speed of 24,000 rpm. The tension in this case was approximately 42,000 lb/in^2 which represents the maximum in terms of the rotor dimension and speed anticipated for this device. Several high strength alloys, similar to those used in rotor blades of jet turbines, are available with tensile strengths well in excess of the calculated operating maximum.

2. Pressure Rise at Rotor Periphery

The ideal pressure rise at the periphery of the rotor may be calculated from equation 2 in which p_3 is the peripheral pressure rise, N is the rotor speed, ρ_a is the density of air, r_o is the radius of the rotor shaft and r_3 is the outer rotor radius

$$p_3 = \frac{4\pi^2 N^2 \rho_a}{g_c} \int_{r_o}^{r_3} r \, d \, r \qquad (2)$$

Assuming a design configuration such that the dust laden air is introduced through a vertical rotor shaft and centrifuged to the rotor periphery, r_3, the air stream then reverses and returns radially against the applied centrifugal force to r_4 where the clean air is exhausted. The above equation may then be used to calculate the ideal pressure rise p_4 at the cleaned air outlet if, instead of integrating to r_3, the integration is carried to r_4, the radius corresponding to the clean air outlet. Table I gives the ideal pressure rise at the rotor periphery and clean air outlet for various rotor speeds.

TABLE I

CALCULATED PRESSURE RISES

Rotor Speed (RPM)	Pressure Rises	
	Peripheral, p_3 (cm of H_2O)	Outlet, p_4 (cm of H_2O)
6,000	37.4	4.8
9,000	84	10.8
12,000	150	19.2
15,000	234	30.0

3. Theoretical Capacity and Flow Conditions

The basic design configuration described in the previous section was used as the basis for capacity calculations. The air inlet was assumed to be one inch in diameter and the spacing between the middle and lower rotor assumed to be 4 cm at the periphery of the middle rotor which was taken to be 10 cm. Table II then lists the inlet air velocity u_1, the internal velocity in the rotor at the point of flow reversal u_2 and the resulting volumetric flow rate.

TABLE II

CALCULATED VOLUMETRIC FLOW RATES AND VELOCITIES

Inlet Velocity, u_1 (m/sec)	Internal Velocity, u_2 (cm/sec)	Volumetric Flow Rate (liters/sec)
0.5	1	0.25
1.0	2	0.50
2.5	5	1.25
5.0	10	2.51
10.0	20	5.02
25	50	12.50
50	100	25.10

4. Sludge Discharge Rates

Several small holes are assumed to be present at the lower rotor periphery for the purpose of discharging accumulated sludge. The flow capacity through one of these holes can be calculated from equation 3 in

which Q is the discharge volumetric flow rate, C is the discharge coefficient, A is the area of one of the holes, g is the gravitational constant, Δp is the pressure drop through the hole, and γ_a is the density of the discharging fluid.

$$Q = CA\sqrt{\frac{2g\ \Delta p}{\gamma_a}} \qquad (3)$$

As a typical example, if the discharging material is assumed to be essentially air and a representative pressure drop of 100 cm H_2O is chosen with a discharge coefficient of 0.6 and a hole diameter of 1/32 inch, the flow rate is 150 $cm^3/sec/hole$. The holes will purposely be of small diameter to restrict air flow. Four such holes should be sufficient to discharge all of the collected material with very little loss of air.

B. Limiting Particle Sizes for Collection in Inclined Radial Paths

The maximum size particle that can pass uncollected along an inclined radial path in a centrifugal separator with inward flow may be estimated. Figure 1 is a schematic representation of the system under consideration. The particle is assumed to be very small so that the inertia of the particle may be neglected and it may further be assumed to obey Stokes' drag forces. From the standpoint of particle equilibrium the following equation is derived

$$u_r = u\cos\alpha = v = \frac{(\rho_p - \rho_1)\ \delta^2\ r\ \omega^2}{18\mu} = \frac{4\pi^2\ (\rho_p - \rho_1)\ \delta^2\ r\ N^2}{18\mu} = \beta\ r\ \delta^2 \qquad (4)$$

where $\beta = [2\pi^2\ (\rho_p - \rho_1)\ N^2]/9\mu$, and u_r is the radial velocity of a particle, u is the instantaneous velocity along the path, v is the instantaneous velocity component perpendicular to the path, α is the angle of

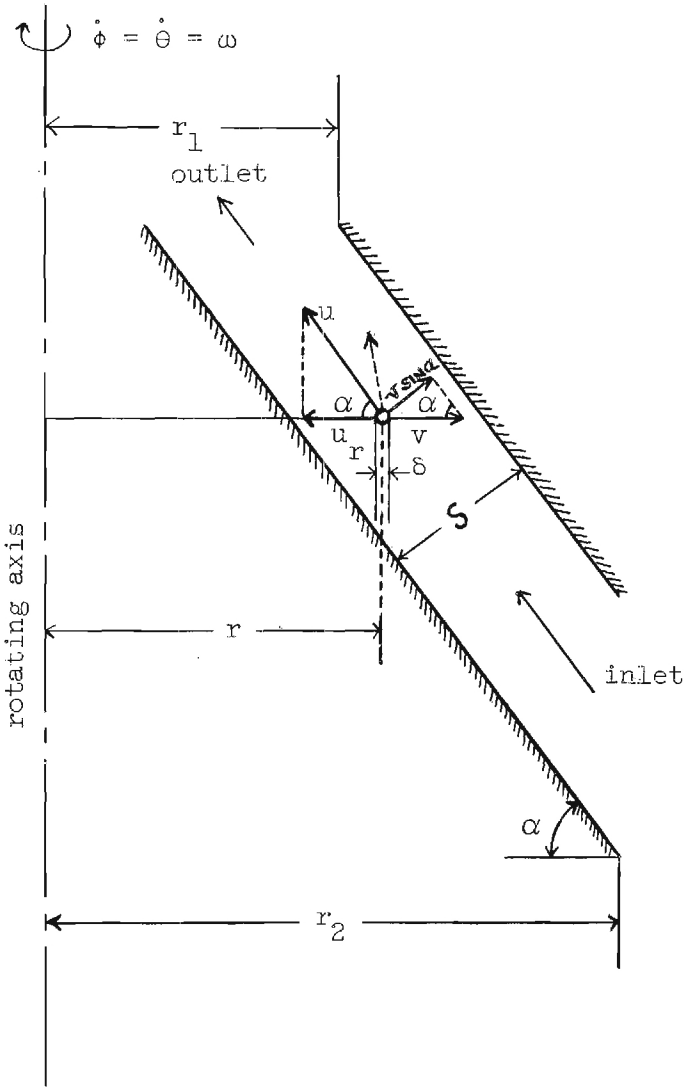

Figure 1. A Particle in an Inclined Radial Path.

path inclination, ρ_p and ρ_l are the densities of the particle and fluid, respectively, δ is the particle diameter, r is the radius of rotation, ω is the angular velocity, μ is the fluid viscosity, and N is the rotor speed in rpm. Rearranging equation 4 gives

$$\delta = \sqrt{\frac{u \cos \alpha}{\beta r}} = \delta_o \sqrt{\cos \alpha} \qquad (5)$$

where δ_o is the cut diameter or maximum uncollected particle diameter in a non-inclined radial path. The velocity u may now be expressed as the quotient of the volumetric flow rate Q and the cross-sectional area of flow (2π rS) giving

$$u = \frac{Q}{2\pi r S} = \frac{c}{r} \qquad (6)$$

Then

$$\delta_o = \sqrt{\frac{\mu}{\beta r}} = \frac{1}{r}\sqrt{\frac{c}{\beta}} \qquad (7)$$

The minimum equilibrium particle size is thus at the rotor periphery. The maximum size of uncollected particles then may be calculated from the following equations which were derived from a force balance on the particle:

$$\frac{-\,dr}{u \cos \alpha - v} = \frac{dS}{v \sin \alpha} = dt \qquad (8)$$

or

$$dS = \frac{v \sin \alpha \cdot dr}{v - u \cos \alpha} = \left[\frac{\beta r \delta^2 \sin \alpha}{\beta r \delta^2 - \frac{c}{r} \cos \alpha}\right] dr = \left[\frac{\beta \delta^2 \sin \alpha \cdot r}{\beta \delta^2 r^2 - c \cos \alpha}\right] dr$$

Integrating this from r_1 to r_2 gives

$$S = \sin \alpha \left[r_1 - r_2 + \frac{1}{\xi \delta} \left(\tanh^{-1} \xi r_2 \delta - \tanh^{-1} \xi r_1 \right) \right] \qquad (9)$$

or

$$\left[\frac{S}{\sin \alpha} + r_2 - r_1 \right] \xi \delta = \tanh^{-1} \xi r_2 \delta - \tanh \xi r_1 \delta \qquad (10)$$

where

$$\xi = \frac{\beta}{c \cos \alpha}$$

The cut diameter δ can be evaluated for given conditions from the above equation by a trial and error process. Jurry and Locke[1] in a study of disk centrifuges have derived an expression equivalent to equation 9 above.

The following typical examples are presented to indicate several limiting cases. For the case of constant velocity at a specified radius, i.e., u = 10 cm/sec at r = 10 cm, with ρ_p = 2.5 gm/cm^3, N = 12,000 rpm, μ = 0.00018 g/cm sec, $\alpha = 30^\circ$ and r_1 = 5 cm, then equation 10 reduces to

$$3780 \, (2S + 5) \, \delta = \tanh^{-1} 37{,}800 \, \delta - \tanh^{-1} 18{,}900 \, \delta$$

Figure 2 and Table III show the calculated results of cut diameter as a function of path height for various volumetric flow rates.

---

1. S. H. Jurry and W. L. Locke, "Continuous Centrifugation in a Disk Centrifuge," A.I.Ch.E. Jnl. 3, p. 480-5 (1957).

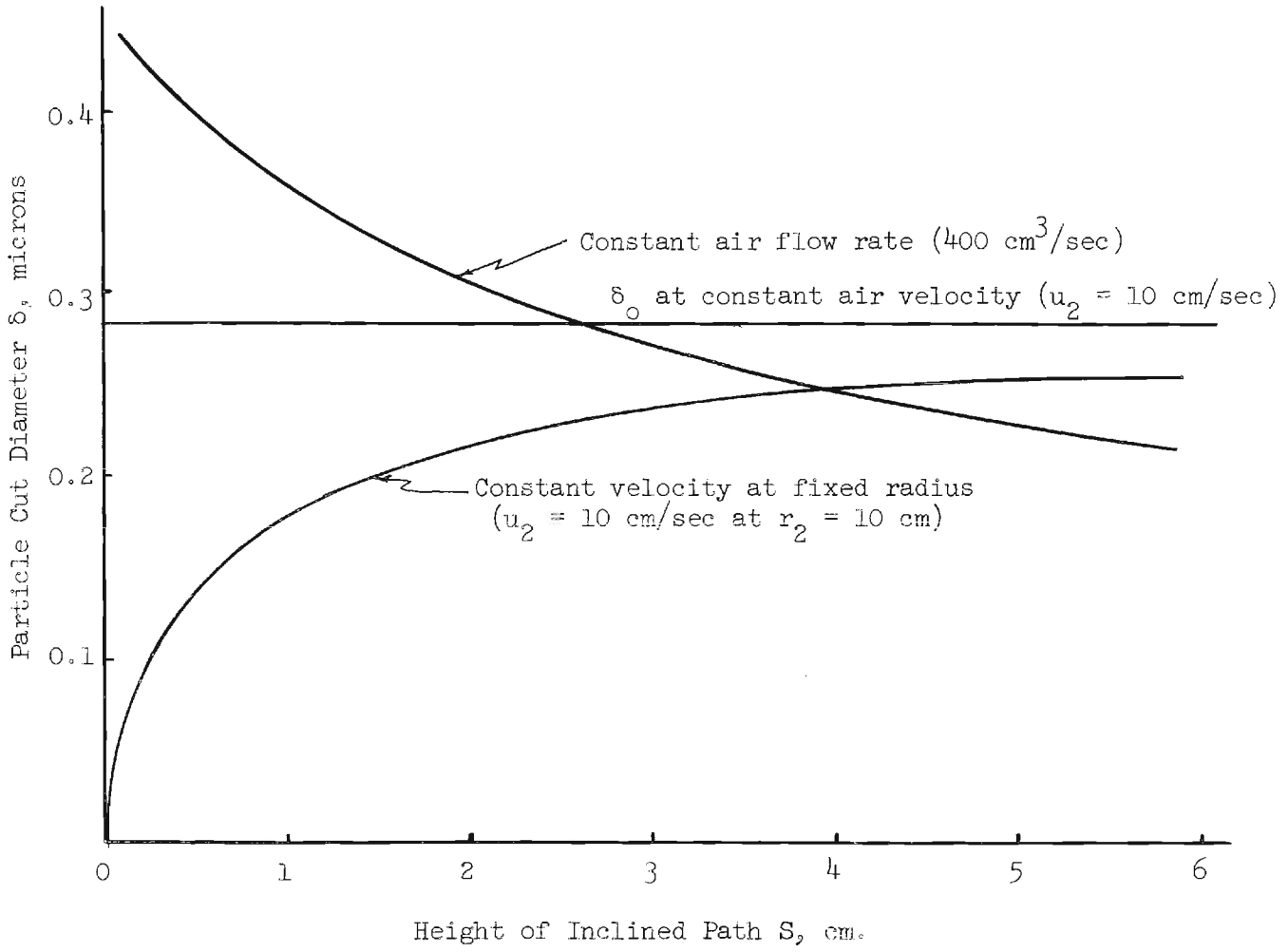

Figure 2. Particle Cut Diameter and Path Height as a Function of Flow Rate and Velocity.

TABLE III

CUT DIAMETER AND PATH HEIGHT OF AN INCLINED RADIAL CHANNEL AT VARIOUS VOLUMETRIC FLOW RATES

Path Heights, S (cm)	Cut Diameter, δ (micron)	Volumetric Flow Rate, Q (liters/sec)
5.35	0.255	3.36
4.00	0.25	2.52
2.00	0.22	1.26
1.00	0.18	0.63
0.60	0.15	0.38
0.24	0.10	0.15
0.07	0.05	0.44

For the case of a constant volumetric flow rate, i.e., $Q = 2\pi k$ = constant, with the same general conditions as given in the preceding case except now Q = 2.52 l/sec, equation 9 reduces to the following

$$1887\ (2\pi + S)\ \sqrt{S}\ \delta = \tanh^{-1}\ 18{,}770\sqrt{S}\ \delta + \tan^{-1}\sqrt{S}\ \delta$$

Calculated results of cut size and path height are also presented in Figure 2 and Table IV for various flow velocities.

TABLE IV

CUT DIAMETER AND PATH HEIGHT OF AN INCLINED RADIAL CHANNEL AT VARIOUS VELOCITIES

Path Heights, S (cm)	Cut Diameter, δ (micron)	Velocity (cm/sec)
6.0	0.21	6.70
4.0	0.25	10.00
2.0	0.31	20.00
1.0	0.36	40.00
0.50	0.40	80.00
0.25	0.42	100.00
0.10	0.44	400.00

The smaller values of S, the height of the channel, naturally create rather high velocities. The cut diameter changes only slightly, however, for large variations in velocity; for example, when the velocity is increased by a factor of 60 the cut diameter increases only by a factor of two and the resulting particle Reynolds Number is not unduly increased. Thus a rather narrow path height is favorable from the standpoint of cut diameter and Reynolds Number as well as for the more uniform fluid velocity profiles associated therewith.

If the fluid velocity along the entire radial path is now assumed constant as would be the case for an inclined radial hole, the integration of equation 8 may be represented by the following:

$$u = \frac{Q}{2\pi r S} = \frac{c}{r} = \text{constant}$$

Then from equation 8

$$dS = \frac{\beta \delta^2 \sin \alpha \, r \, d \, r}{\beta \delta^2 r - u \cos \alpha}$$

Now, integrating from r_1 to r_2,

$$S = \sin \alpha \left[r_1 - r_2 + \frac{u \cos \alpha}{\beta \delta^2} \ln \frac{\frac{u \cos \alpha}{\beta \delta^2} - r_1}{\frac{u \cos \alpha}{\beta \delta^2} - r_2} \right] \qquad (11)$$

or

$$\frac{S}{\sin \alpha} + r_2 - r_1 = \frac{1}{(\xi r) \delta^2} \ln \frac{1 - (\xi^2 r) \delta^2 r_1}{1 - (\xi^2 r) \delta^2 r_2} \qquad (12)$$

With the same experimental conditions as used in the first example, except now the calculations are for a hole of constant radius instead of converging radial flow, equation 12 reduces to

$$(2S + 5) + \frac{1.614}{\delta^2} \log_{10} \frac{0.1404 - \delta^2}{0.1404 - 2\delta^2}$$

Table V and Figure 3 give typical values of cut diameters for varying hole diameters.

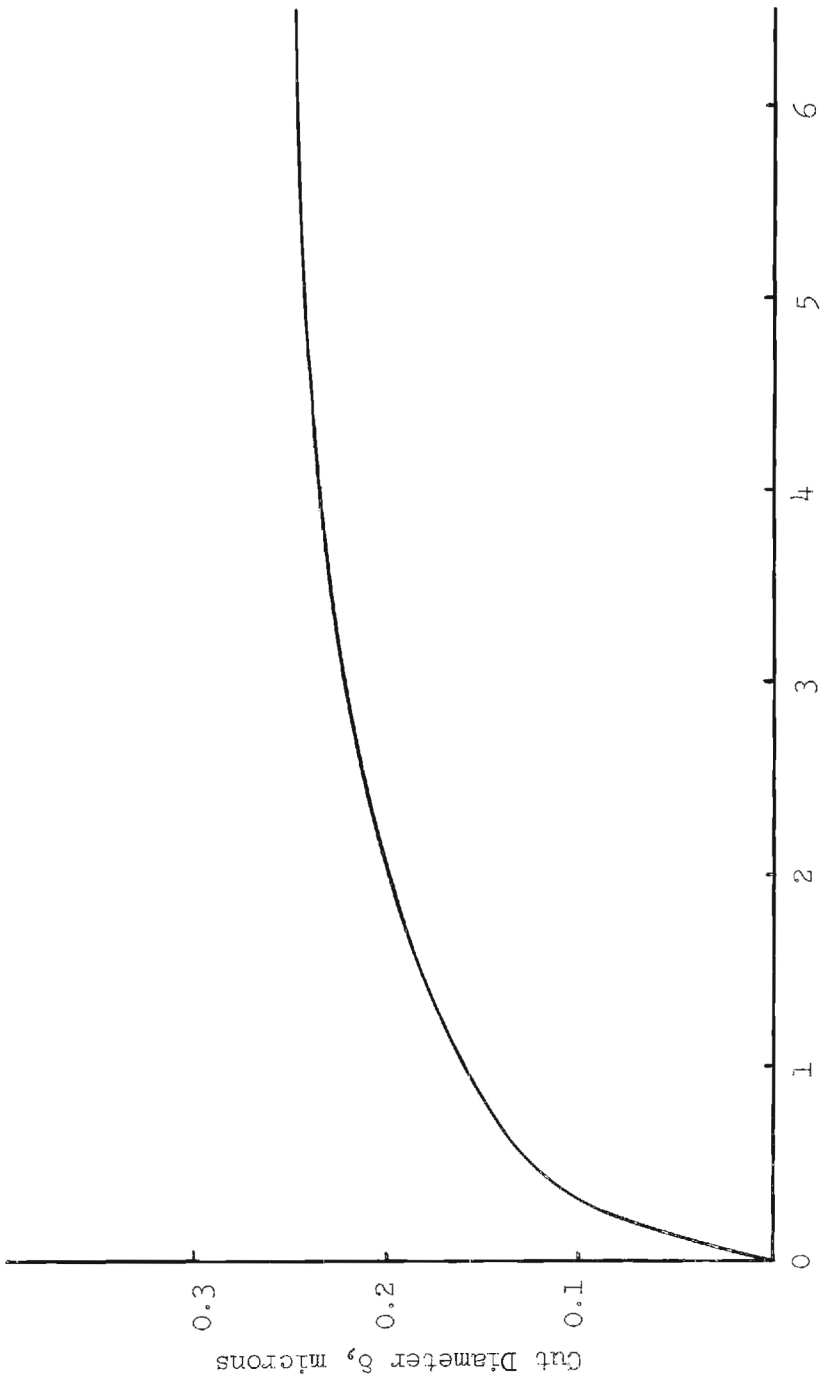

Figure 3. Particle Cut Diameter and Path Height for a Constant Air Velocity (u = 10 cm/sec).

TABLE V

CUT DIAMETER ATTAINED IN INCLINED RADIAL HOLES
OF VARYING DIAMETER

Path Heights, S (cm)	Cut Diameter, δ (micron)
6.60	0.25
1.96	0.20
0.81	0.15
0.30	0.10
0.14	0.05

A further calculation from equation 12 for a constant cut diameter of 0.25 micron gives Table VI showing flow velocities for varying hole diameters.

TABLE VI

FLOW VELOCITIES FOR VARIOUS HOLE DIAMETERS
AND A FIXED CUT DIAMETER

Hole Diameter, S (cm)	Flow Velocity, u (cm/sec)
10	6.60
20	1.28
40	0.50
100	0.14

C. Particle Classification by Size

Particle movement in a fluid while subjected to a centrifugal field, such as prevails in centrifugal separators and classifiers, has generally

been considered in terms of a steady state, terminal velocity for reasons of mathematical simplicity. A centrifugal force in a separator or classifier continuously changes with changing radius, however, so that a particle may never truly attain terminal conditions. While the steady state approach is generally adequate for calculations of limiting effects such as separation cut diameter, it is completely inadequate for accurate calculation of particle trajectories. In order to predict accurately trajectories of particles subjected to strong centrifugal fields for short periods of time (on the order of 10^{-3} sec) the motion of a particle should be considered in terms of particle inertia in the radial and tangential directions allowing for tangential and radial slip between particle and fluid.

A particle moving in a fluid is decelerated by the action of frictional forces and it may be accelerated by the action of external influences. The resultant force acting on a particle in any direction will be the vectorial sum of the frictional and external forces. The frictional drag acting on the particle will depend inherently on the instantaneous velocity of the particle. In the laminar flow region, the drag forces may be represented by Stokes[2] law. At higher flow rates, turbulent flow prevails and the drag coefficient is approximately constant. If the diameter of the particle is comparable in magnitude to the mean free path of the fluid molecules, the drag coefficient has lower values than predicted by Stokes' law and a correction factor such as developed

2. G. C. Stokes, "Mathematical and Physical Papers," Trans. Cambridge Phil. Soc. 9, Part II, 101-9 (1901).

by Cunningham[3] must be applied.

By the methods of vector analysis, the following two-dimensional equations describe the motion of a spherical particle undergoing simple rotational motion in the laminar flow region in the absence of a gravitational field

$$\frac{d^2r}{dt^2} + a\frac{dr}{dt} - r\left(\frac{d\theta}{dt}\right)^2\left[1 - \frac{\rho_f}{\rho_p}\left(\frac{d\phi}{d\theta}\right)^2\right] = 0 \qquad (13)$$

$$r\frac{d^2\theta}{dt^2} + ar\left(\frac{d\theta}{dt} - \frac{d\phi}{dt}\right) + 2\frac{dr}{dt}\frac{d\theta}{dt} = 0 \qquad (14)$$

where a is equal to $(18\mu)/[(\rho_p - \rho_f)\,\delta^2]$, μ is the fluid viscosity, δ is the particle diameter, ρ_f is the density of fluid, ρ_p is the density of particle, r is radius of revolution, t is time, $d\phi/dt$ is the angular velocity of fluid, and $d\theta/dt$ is the angular velocity of particle.

These general equations are too complex to solve in general form and direct integration can be performed only for special cases. For example the equations have been solved with certain simplifying assumptions for the case of a forced vortex. These solutions are compared with exact solutions as obtained with an analog computer. Figure 4 is a plot of these solutions.

The angular velocity of the fluid is defined according to the type of centrifugal field and, for the case of a forced vortex, is a constant.

---

3. E. Cunningham, "On the Velocity of Steady Fall of Spherical Particles through Fluid Media," Proc. Royal Soc. 83A, 357-65 (1910).

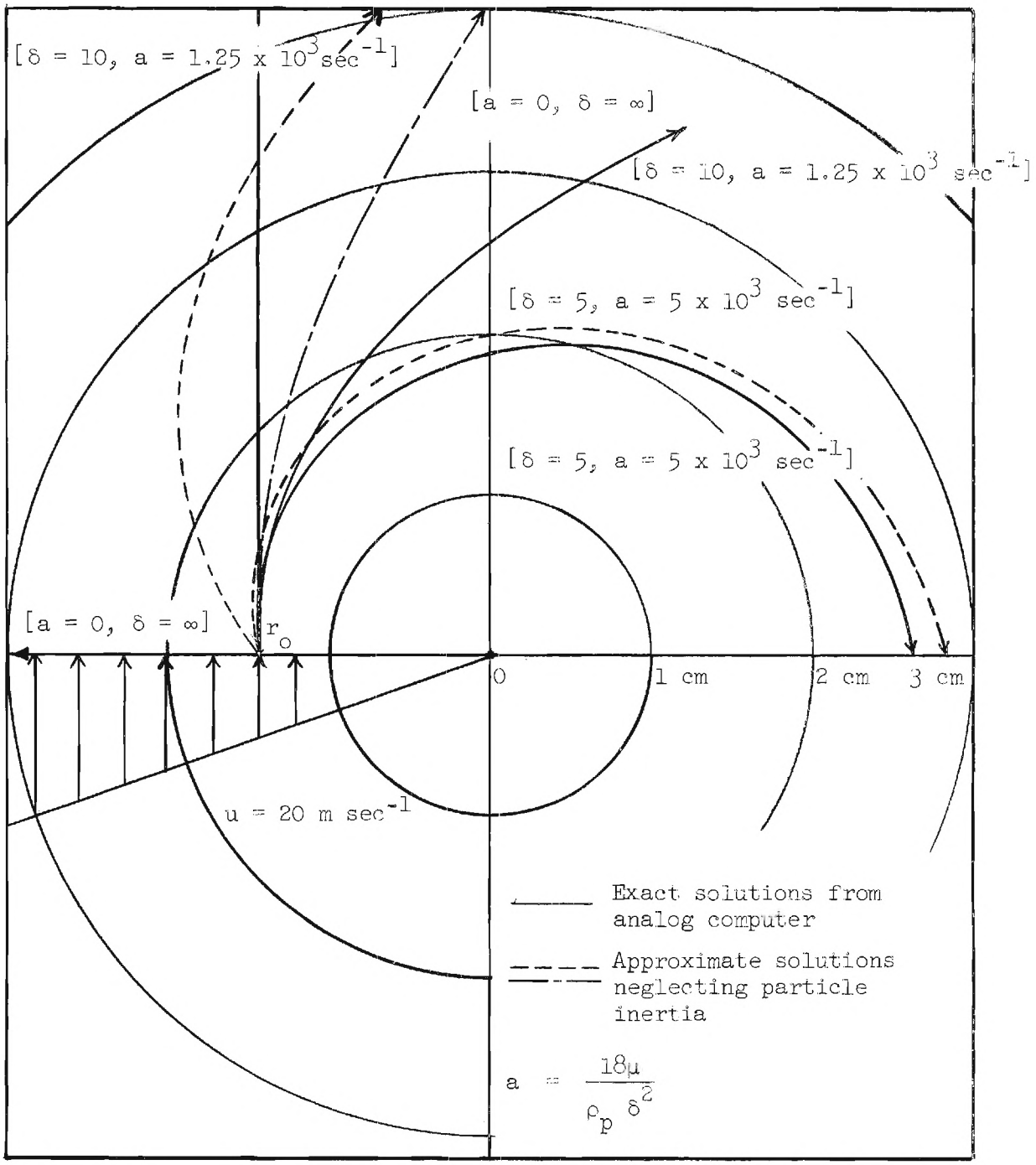

Figure 4. Calculated Particle Trajectories in a Forced Vortex Field ($\omega = 10^3$ sec^{-1}, $\rho_p = 2.6$ gms/cm^3).

Under these conditions and with the assumption that the particle density is much greater than the fluid density, the general equations reduce to

$$\frac{d^2r}{dt^2} + a\frac{dr}{dt} - r\left(\frac{d\theta}{dt}\right)^2 = \text{(assuming } \rho_p \gg \rho_f\text{)} \tag{15}$$

and

$$r\frac{d^2\theta}{dt^2} + ar\frac{d\theta}{dt} - acr + 2\frac{dr}{dt}\frac{d\theta}{dt} = 0, \tag{16}$$

where $d\phi/dt$ is a constant c.

If the assumption is made that there is no tangential slip between particle and fluid, i.e., $d\phi/dt = d\theta/dt$, then equations 15 and 16 reduce to

$$\frac{d^2r}{dt^2} + a\frac{dr}{dt} - rc^2 = 0. \tag{17}$$

The solution of equation 17 when $t = 0$, $\phi = 0$, $\theta = 0$, $r = r_o$, and $dr/dt = 0$, is

$$r = r_o e^{-\frac{a}{2}t}\left[\cosh\sqrt{\frac{a^2}{4}+c^2}\;t + \frac{a}{2\sqrt{\frac{a^2}{4}+c^2}}\sinh\sqrt{\frac{a^2}{4}+c^2}\;t\right] \tag{18}$$

and

$$\frac{dr}{dt} = r_o e^{-\frac{a}{2}t}\left[\frac{c^2}{\sqrt{\frac{a^2}{4}+c}}\sinh\sqrt{\frac{a^2}{4}+c^2}\;t\right] \tag{19}$$

If the inertia of the particles is neglected and the preceding assumptions are still allowed, equation 17 reduces to

$$a \frac{dr}{dt} = rc^2 \tag{20}$$

and

$$r = r_o e^{\frac{c^2}{a} t} \tag{21}$$

Therefore

$$\frac{dr}{dt} = \frac{c^2}{a} r_o e^{\frac{c^2}{a} t} \tag{22}$$

Examination of the equations of motion reveals that the movement of a particle in any direction is dependent not only on the velocity component in that direction but also on the resultant velocity. Hence a particle moving radially in a centrifugal field will have a decreased radial component if a tangential fluid stream is incident on the particle in the direction of motion. The particle will not attain its undisturbed radial velocity until it has attained the tangential velocity of the impinging stream. This effect is size dependent as the smaller particles will rapidly approach the tangential fluid velocity whereas the greater inertia of larger particles will result in a lesser effect. The initial conditions of particle motion may thus be readily varied and they have considerable effect on any resulting classification.

IV. DESIGN AND CONSTRUCTION

The first experimental model of the centrifugal separator consisted essentially of a three-component rotor mounted on a hollow, vertical shaft supported by double-sealed precision high speed bearings above and below the rotor. A general cross-sectional view of the centrifugal separator is given in the assembly drawing of Figure 5. Figure 6 is a photograph of the centrifugal separator with the upper housing removed showing the rotor assembly in place. The rotor assembly consisted of three separate rotors constructed from a hand-forged aluminum-zinc alloy, 7075-T6. This alloy is a corrosion resistant high strength material with a minimum tensile strength of 66,000 lb/in^2. Figures 7, 8, and 9 are drawings of each of the rotor components. Figure 10 is a photograph of the rotor components and two different designs of rotor shafts. Rotor assemblies were statically and dynamically balanced for operational speeds up to 18,000 rpm.

The device is equipped with a wash-down jet to introduce water into the top of the rotor assembly which then is forced radially outward by the centrifugal field. As the water flows counter to the clean air, the material deposited on the rotor is scrubbed and discharged through the sludge outlet holes provided in the lower rotor component. The general flow path of air and water can be seen Figure 5. The housing and motor support were constructed of large diameter centrifugally cast steel pipe and hot rolled steel plate. Figure 11 is a general view of the housing unit.

The driving unit for the first experimental design was 1/2 hp electric motor manufactured by the Stanley Electric Tool Division capable of no-load speeds to 22,000 rpm. This first motor had insufficient

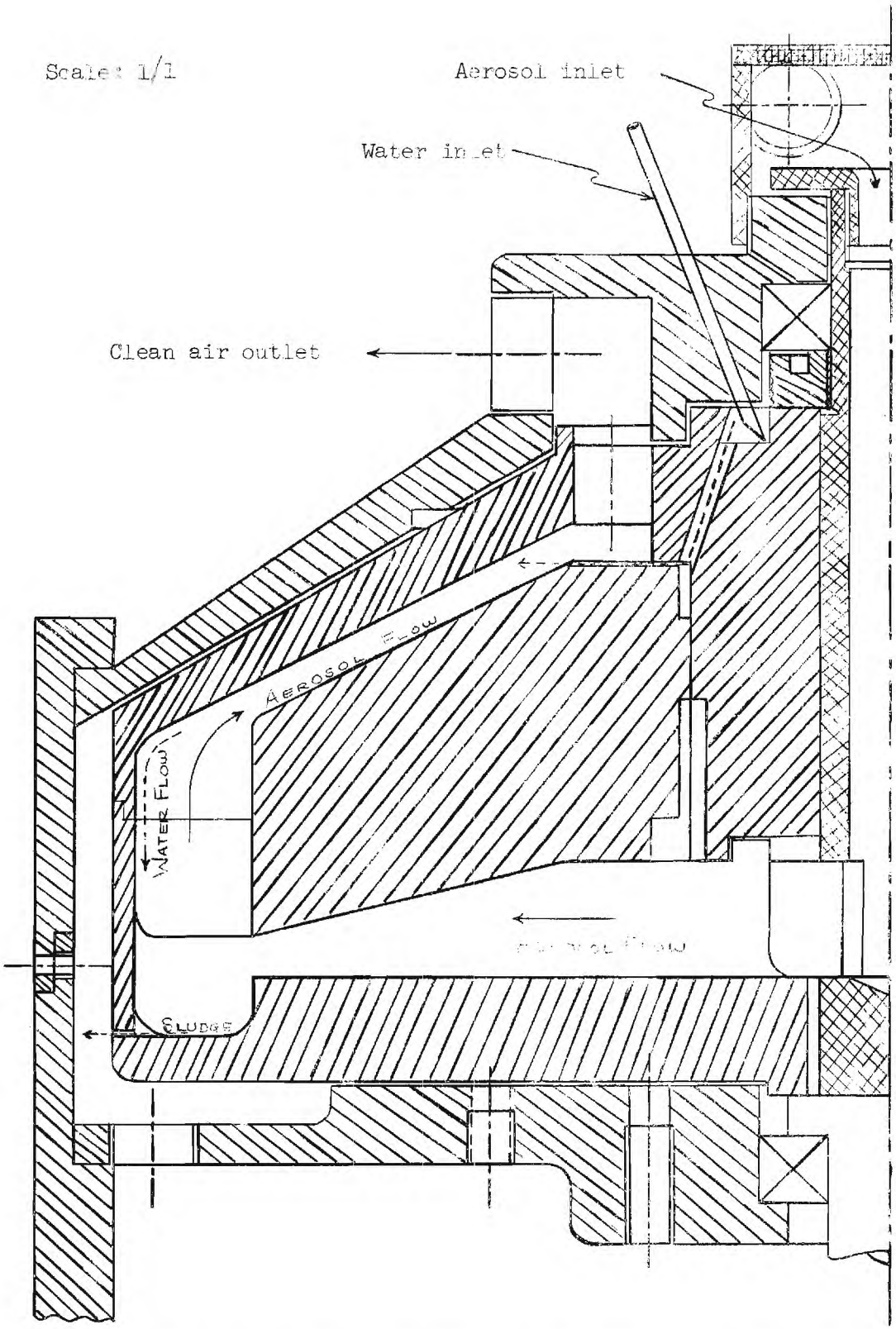

Figure 5. Assembly Drawing of the Centrifugal Separator.

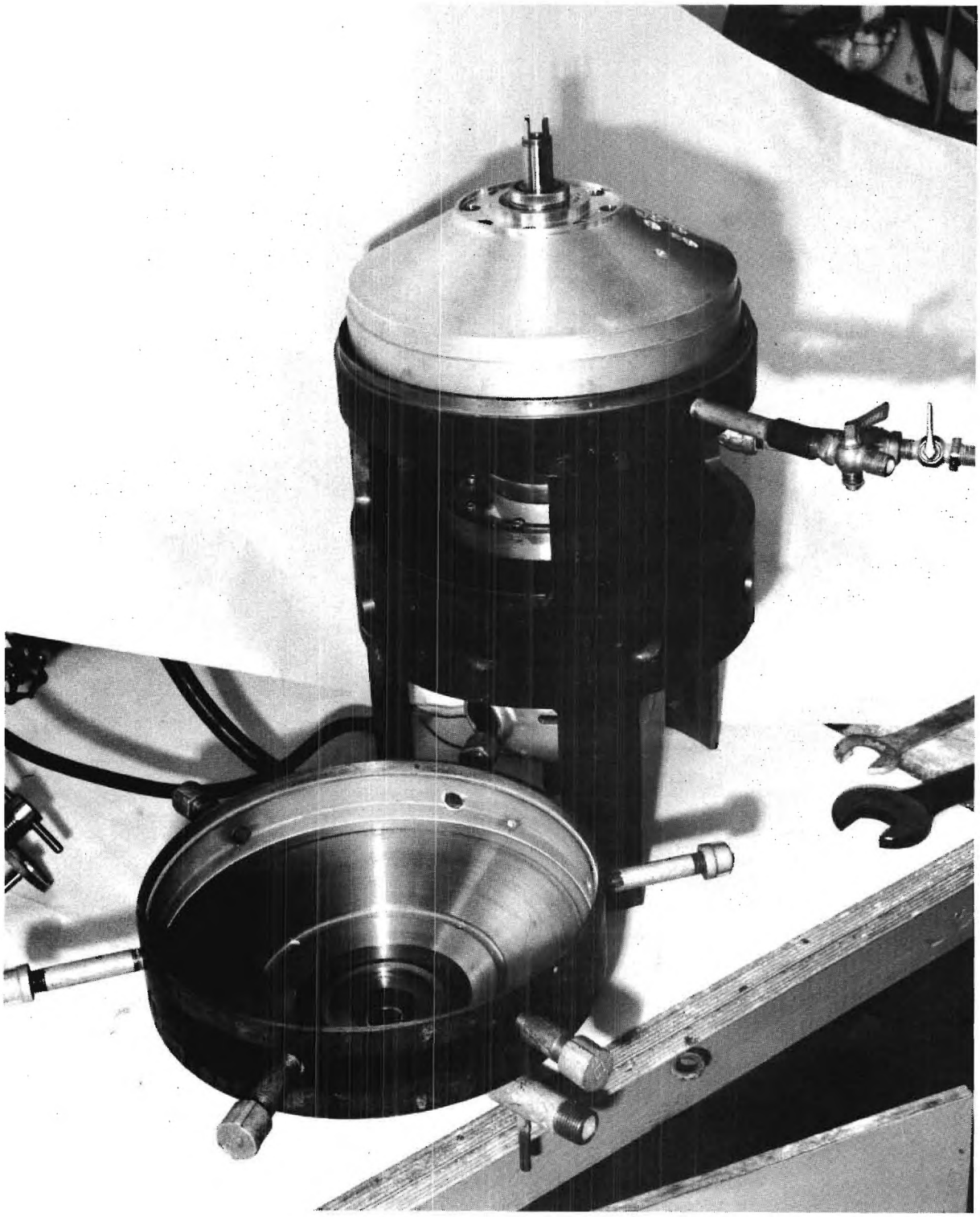

Figure 6. The Centrifugal Separator with the Upper Housing Removed.

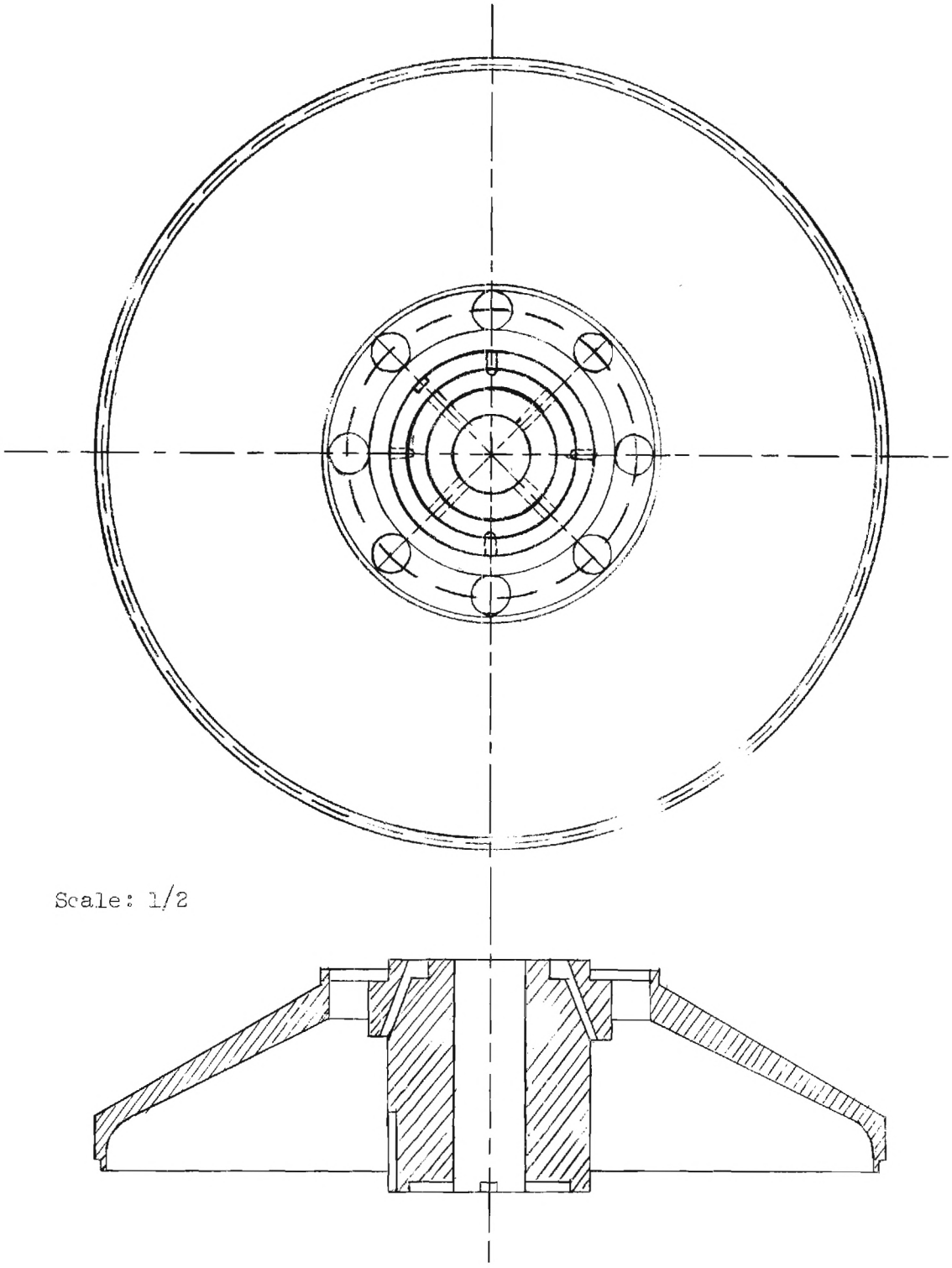

Figure 7. Centrifugal Separator Upper Rotor.

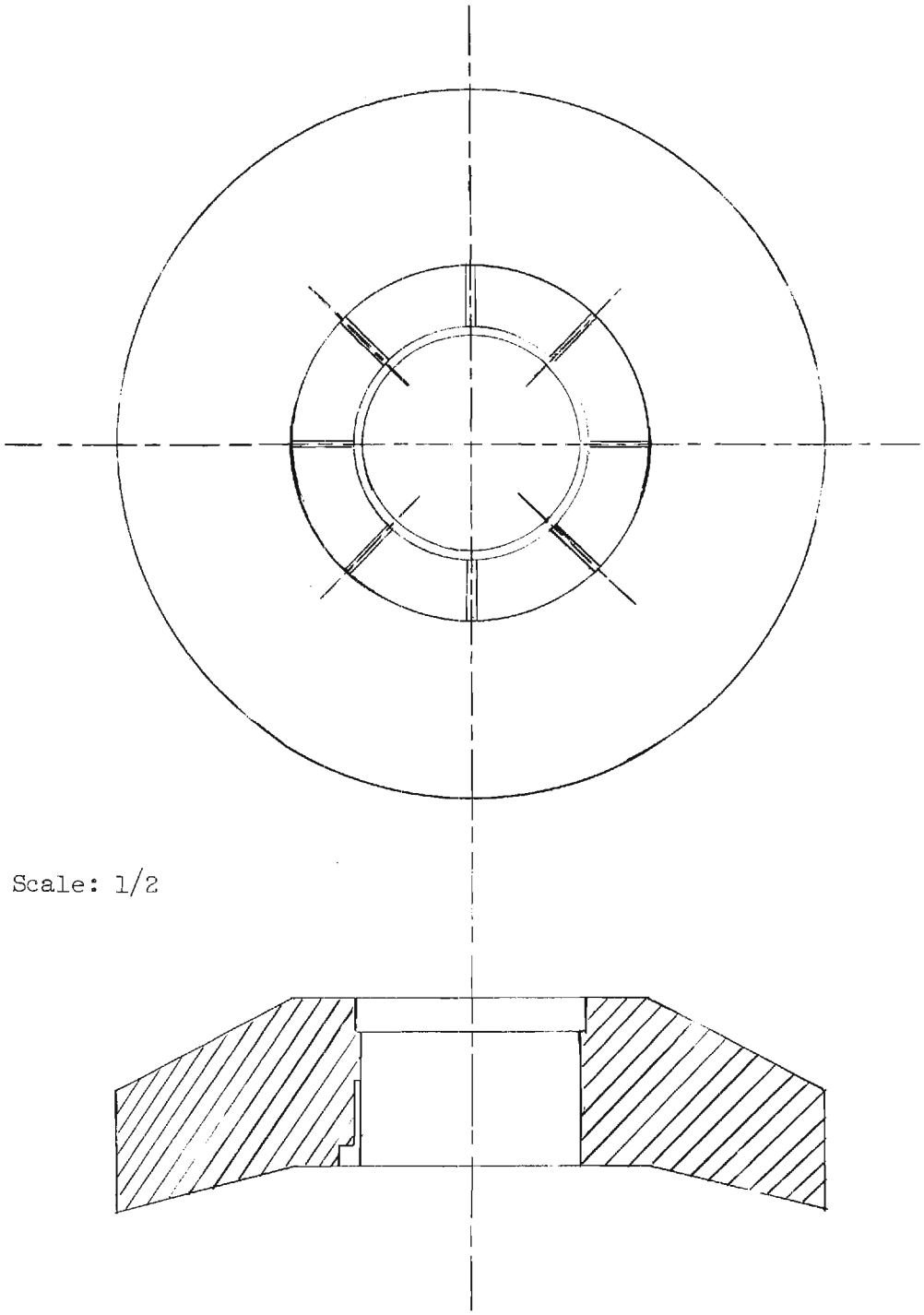

Figure 8. Centrifugal Separator Middle Rotor.

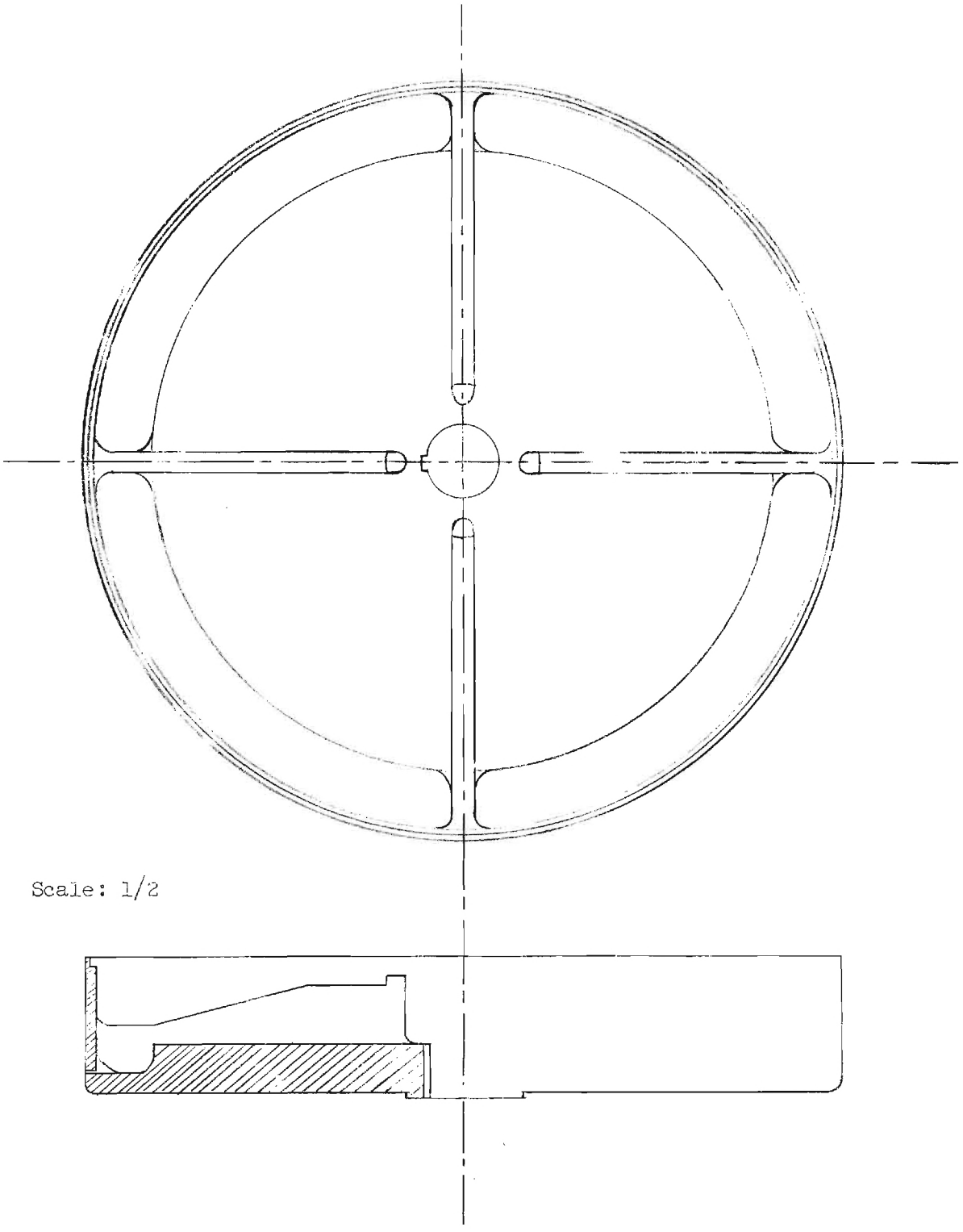

Figure 9. Centrifugal Separator Lower Rotor.

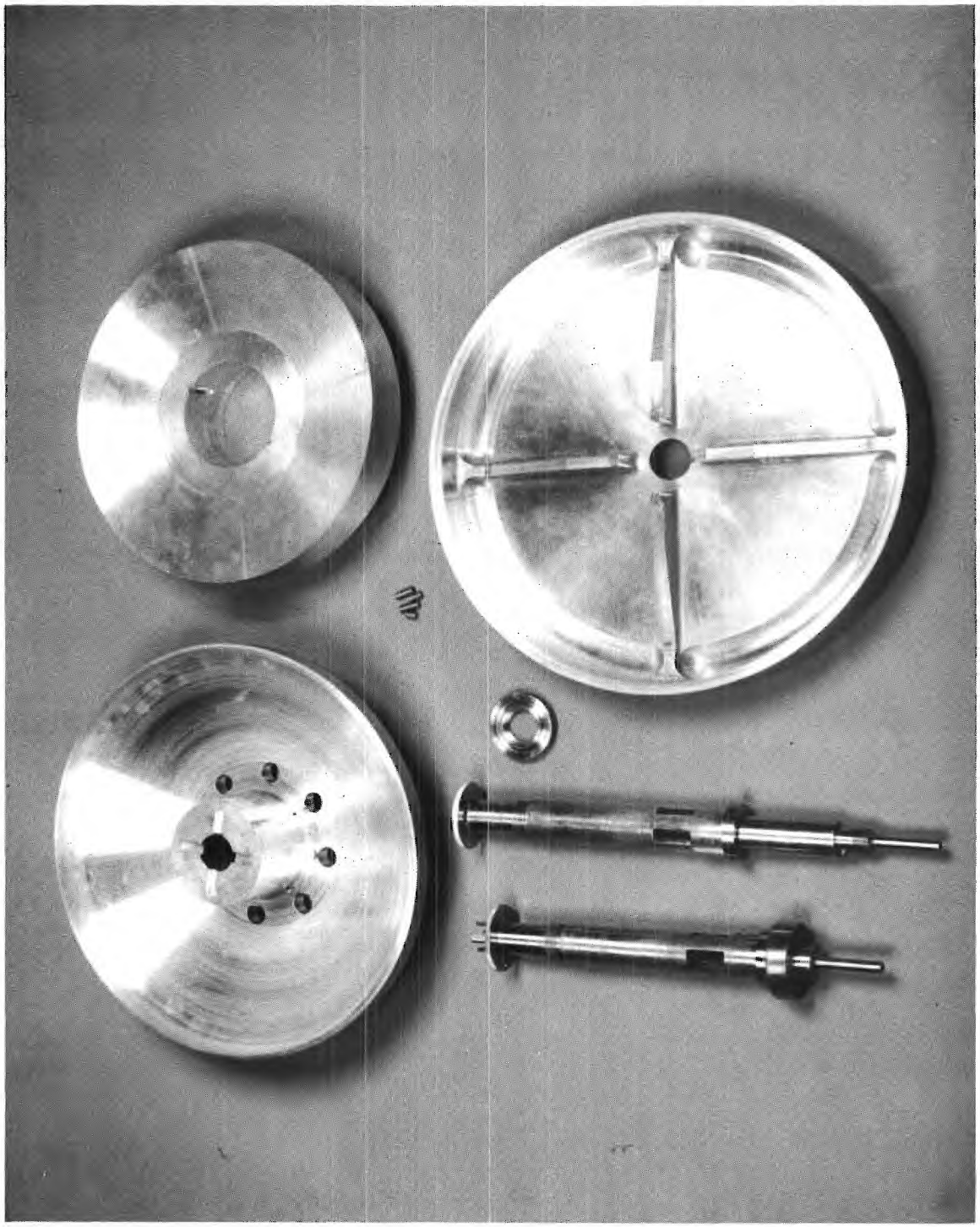

Figure 10. Centrifugal Separator Rotor Components and Shafts.

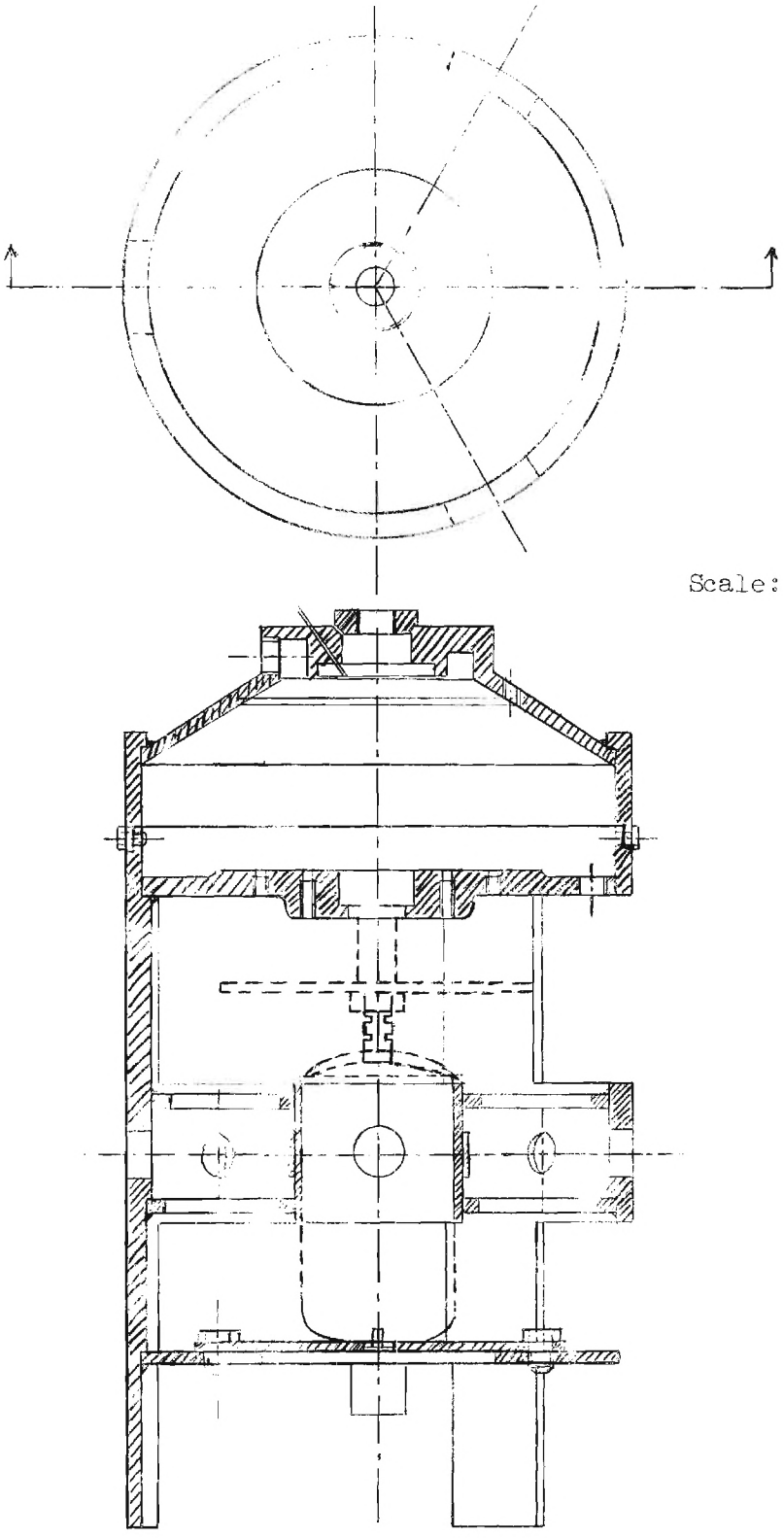

Figure 11. Housing Unit for Centrifugal Separator with Driving Motor No. 1.

torque to provide speeds under load above 8,000 rpm so a second more powerful motor was substituted. This second driving unit was a 2-1/2 hp electric motor manufactured by the Stanley Electric Tool Division capable of no-load speeds to 18,000 rpm and sufficiently powerful to drive the centrifugal separator at speeds in excess of 12,000 rpm.

A second rotor designed especially to study the classification of materials according to particle size is shown in the photograph of Figure 12. Figure 13 is a drawing of the classifier rotor assembly. This rotor assembly was also constructed of the aluminum alloy 7075-T6 and statically and dynamically balanced for operation at speeds to 15,000 rpm. The classifier rotor was designed so that the same housing unit and driving motor could be used for it as for the centrifugal separator. The upper housing unit was slightly modified by adding four additional pressure relief ports to minimize peripheral pressure rise.

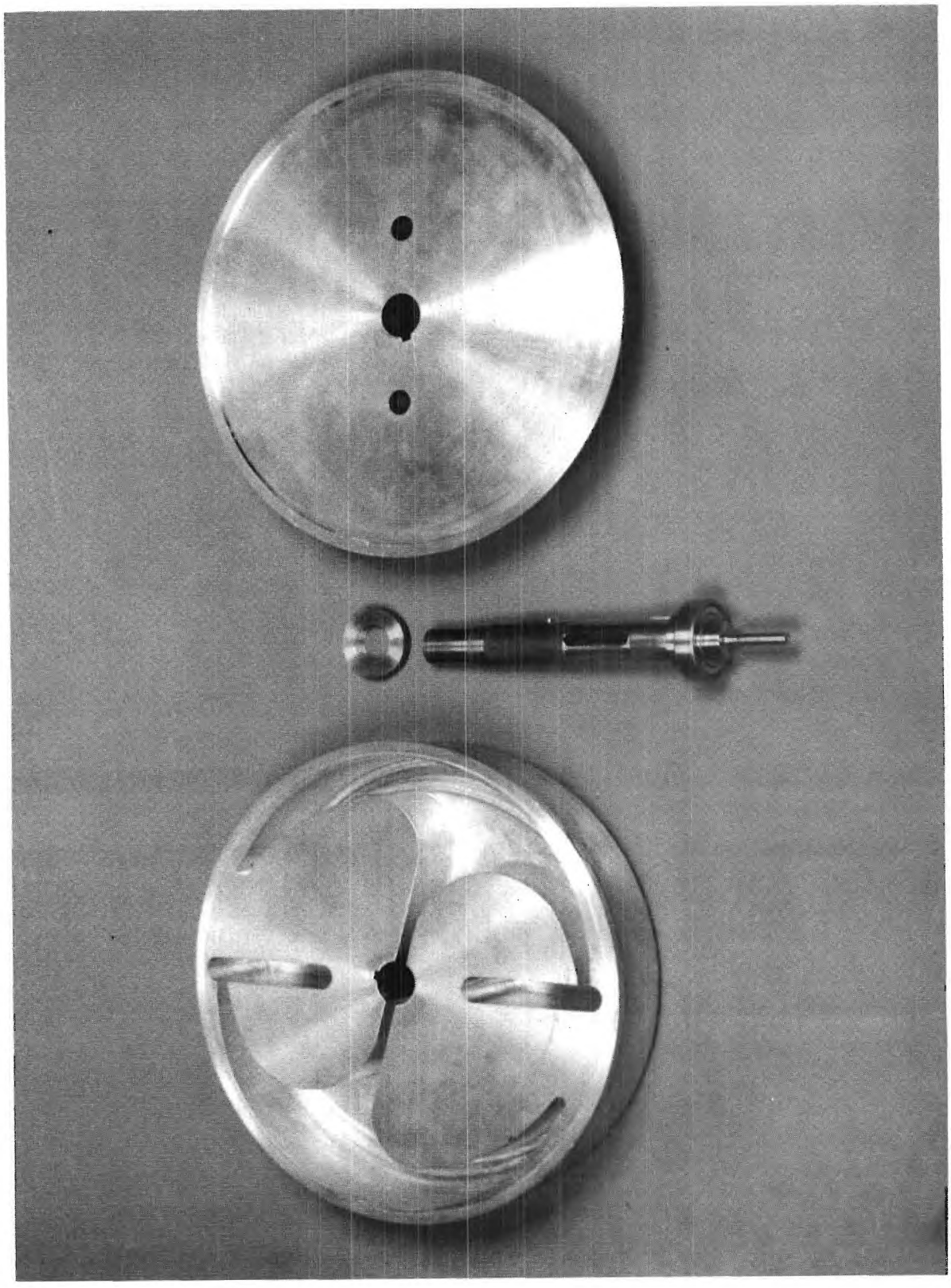

Figure 12. Centrifugal Classifier Rotor Assembly and Shaft.

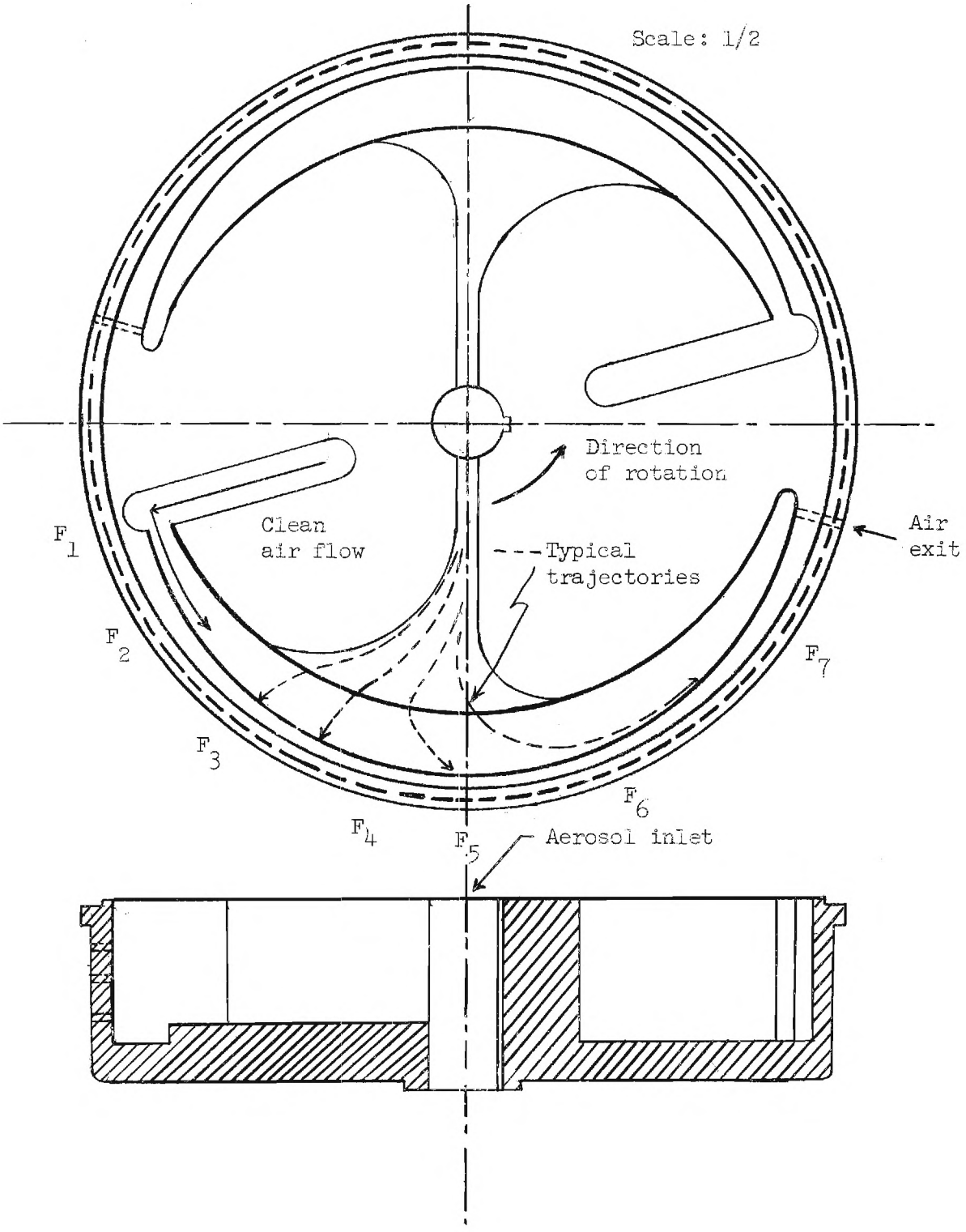

Figure 13. Centrifugal Classifier Lower Rotor.

V. EXPERIMENTAL OPERATION AND RESULTS

A. Centrifugal Separator Procedure

A well dispersed aerosol of known concentration was generated externally and introduced to the centrifugal separator through a feed enclosure surrounding the top of the hollow rotor shaft. The aerosol flowed axially down the rotor shaft to slots provided near the base where it entered into the centrifugal field. The aerosol was accelerated by the centrifugal field toward the periphery of the lower rotor where most of the aerosol particles were impacted onto the wall and there collected. The configuration of the middle and lower rotor provided a converging flow path to stabilize the accelerating flow and promote laminar flow. At the periphery of the middle rotor the flow path reversed and the now more dilute aerosol passed through the inclined radial path formed by the top of the middle rotor and the lower side of the top rotor to the clean air exit. As the dust laden air passed through the inclined radial path counter to the centrifugal field, particle drag and centrifugal force were in direct opposition and many of the smaller particles were deposited onto the lower side of the top rotor. The "clean" air then passed through the exit port to a Goetz Aerosol Spectrometer[4] which was used as an "absolute" collection device to determine the size range and amount of those particles passing uncollected through the centrifugal separator. Figure 14 is a photograph of the experimental setup showing the centrifugal separator with the aerosol generator placed directly above the top of the rotor shaft. Pressure taps were provided at the aerosol inlet,

4. A. Goetz, "An Instrument for the Quantitative Separation and Size Classification of Air-Borne Particulate Matter Down to 0.2 Micron," Proc. II. Int. Symp. Condensation Nuclei, Rev. Geofisica Pura E Applicata 36, 49-69 (1957).

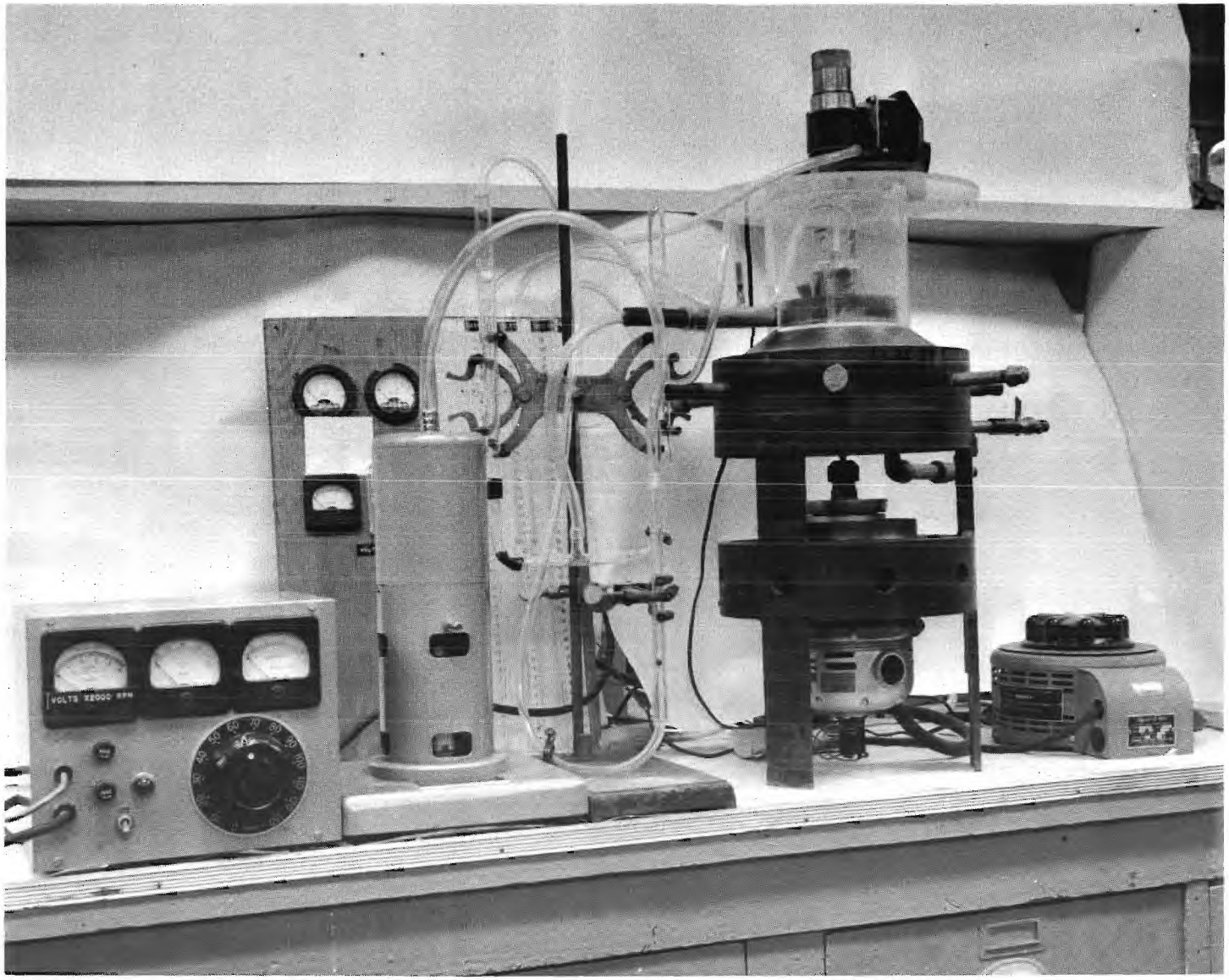

Figure 14. Centrifugal Separator and Auxiliary Equipment.

rotor periphery and clean air exit. The instrument cluster seen in the left background of Figure 14 shows the voltmeter from the tachometer generator on the driving motor, the voltmeter and ammeter which indicate the input voltage and amperage to the driving motor, and the open-end manometers used to measure pressure drops at the points noted previously. The device seen in the left foreground of Figure 14 is the Goetz aerosol spectrometer and control instrumentation.

The separation efficiency of the centrifugal separator was determined by weighing the material collected on the foil liner of the Goetz aerosol spectrometer and then calculating the weight fraction this was of the amount of material fed into the separator. The operation speed of the Goetz spectrometer was adjusted until the centrifugal force generated therein was sufficient to eliminate essentially all of the particles passing into it in about 1/3 of the length of its helical channels. Figure 15 is a photograph of the disassembled Goetz aerosol spectrometer and the centrifugal separator rotor components showing the material that was collected on the centrifugal separator rotor and the plastic film that covered the helical channels of the Goetz spectrometer. Figure 16 also shows the disassembled centrifuged separator rotor with areas of particle deposit more clearly visible.

Experimental runs were generally 30 minutes to 1 hour in duration with aerosols containing 0.003 to 0.03 gm/liter of solids at varying volumetric flow rates. Operation speeds of the separator varied from 2000 to in excess of 12,000 rpm. Several runs of 3 hours duration were made in which water was injected every 30 minutes in sufficient

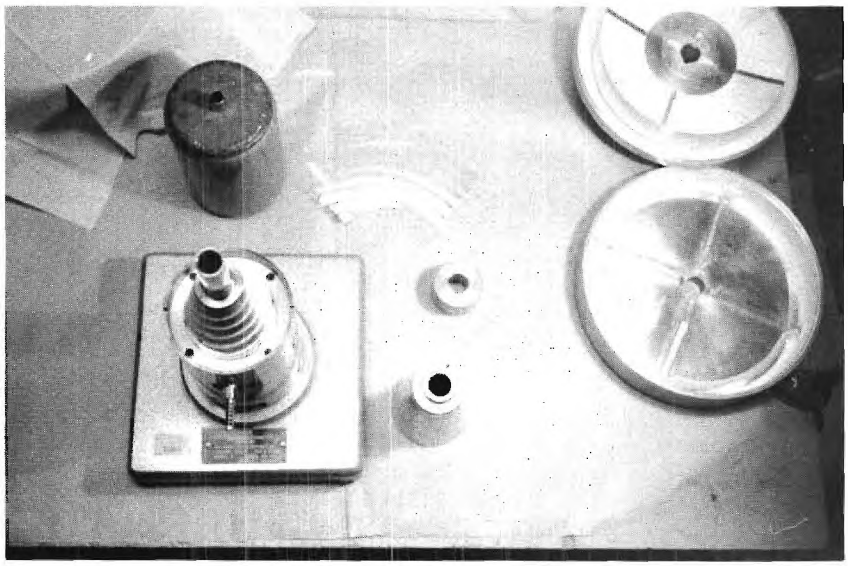

Figure 15. Material Collected on Centrifugal Separator Rotors and Goetz Spectrometer Film.

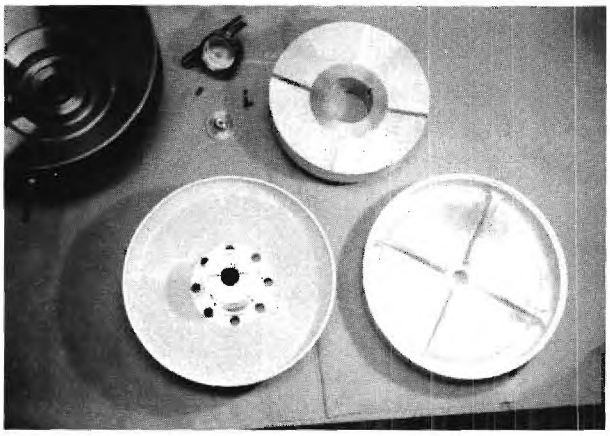

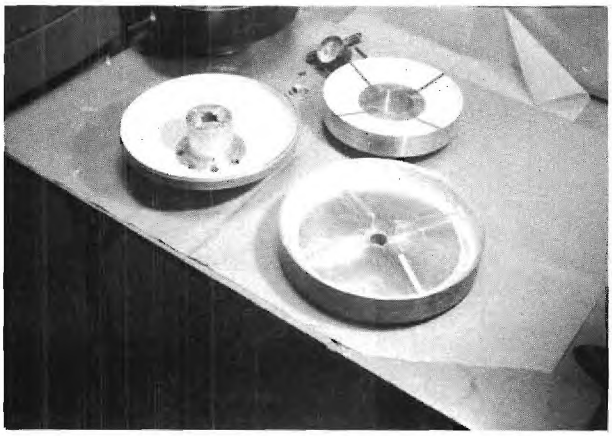

Figure 16. Material Collected on Centrifugal Separator Rotors.

quantity to wash down the collected solids. The operation speed was reduced to 2000 rpm during wash down to minimize the increased stresses created by the weight of sludge and water.

B. Centrifugal Classifier Procedure

A Wright dust feeder[5] or similar devices were used to generate an aerosol of the material to be classified. This aerosol was then introduced to the centrifugal classifier through a feed enclosure surrounding the top of the hollow rotor shaft. The aerosol flowed down the rotor shaft to a plastic feed jet built into the rotor shaft. This arrangement created essentially a point entry port for the aerosol particles into the classifier. Typical trajectories of particles are shown in the plan view of the lower classifier rotor previously presented in Figure 13 on page 33. Once the aerosol particles have entered the centrifugal field they are accelerated to the periphery of the rotor where the combined effects of particulate drag and centrifugal force culminate in the deposition of a continuous, graded spectrum of particles. An additional drag force was imposed on the aerosol particles in some cases by admitting a secondary stream of particle-free air which flowed along the periphery of the rotor in the direction of rotation as can be seen from Figure 13. Orifices of varying diameter could be inserted in the air inlet holes of the top rotor to control the amount of this secondary air flow. The presence of this additional drag force decreased the deposition angle of the smaller particles but had a lesser effect on the larger particles. This effect

5. B. M. Wright, "The Wright Dust Feed Mechanism," Journal of Scientific Inst. 27, No. 1, 12-16 (1950).

enables a rather narrow size distribution to be distributed more widely on the rotor periphery, thereby effecting a more efficient classification. Air and uncollected particles were exhausted to the atmosphere through the air exit holes in the lower rotor. Thin strips of plastic were placed at the periphery of the lower rotor and the classified particles were collected thereon. At the conclusion of a run, the strip was carefully removed from the rotor, examined for deposit characteristics, and particle size distributions were determined at specified intervals along the strip. Test runs were made at various rotor speeds, aerosol flow rates, and secondary air flow rates.

Particle size distributions were determined either microscopically, by the Sharples micromerograph, or by the Coulter counter depending upon the size range and the amount of material available.

C. Experimental Results

1. Centrifugal Separator

The centrifugal separator was evaluated with talc, glass beads, $CaCO_3$, $BaSO_4$ and TiO_2 aerosols. The collection efficiency η for TiO_2 aerosols at various rotor speeds and aerosol flow rates is given in Table VII. The TiO_2 powder used in these studies consisted of 95 per cent by weight of particles less than one micron in diameter and was of a considerably smaller overall size distribution than any of the other materials tested, thus it was more difficult to separate from an air stream than any of the other materials tested. Talc, for example, of a much coarser distribution was collected with an efficiency exceeding 99.9 per cent even at rotor speeds as low as 2000 rpm. Talc particles were also found

to be fairly well classified according to size on the separator rotor as is shown by the size distributions at the locations specified in Figure 17.

2. Centrifugal Separator Power Consumption and Pressure Drop

The power consumption curves for the centrifugal separator with both driving units used is given in Figure 18 as a function of rotor speed. Energy losses due to excessive viscous heating between the rotor and case were at first believed to be a major contributor to the high power consumption. A spacer ring was made to be inserted between the upper and lower housing to increase the clearance between the rotor and upper housing, and the lower housing face was machined off 1/8 inch to increase clearance between the lower rotor and case. No noticeable decrease in power consumption was noted until rotor speeds exceeded 8000 rpm; from this speed upward a decrease of approximately 5 per cent in the power consumption was noted. Apparently much of the power consumption was a result of bearing losses. The bearing system used consisted of two double sealed, lubricated high speed bearings.

3. Centrifugal Classifier

The classifications achieved with talc and with glass beads are shown by the size distributions of Figures 19 and 20. Figures 21 and 22 are micrographs of materials from each size fraction of the distributions indicated. The glass beads used were dispersed by a powder atomizer and no secondary air flow was used; therefore, the fluid conditions within the classifier closely approximated those of a forced vortex. Rotor speed was 4000 rpm for classification of the glass beads with all pressure relief

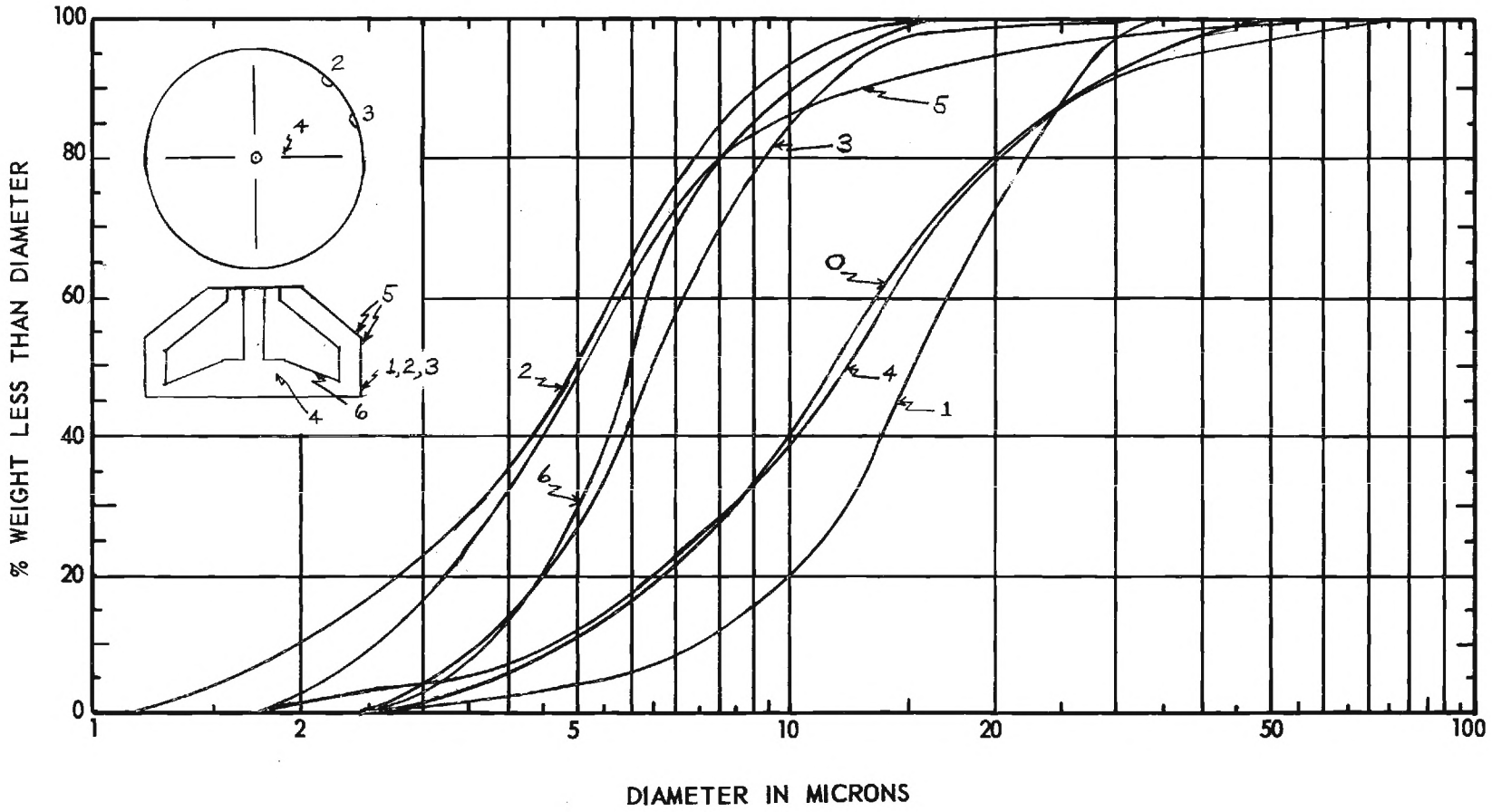

Figure 17. Size Distributions of Talc at Various Positions on the Centrifugal Separator Rotor.

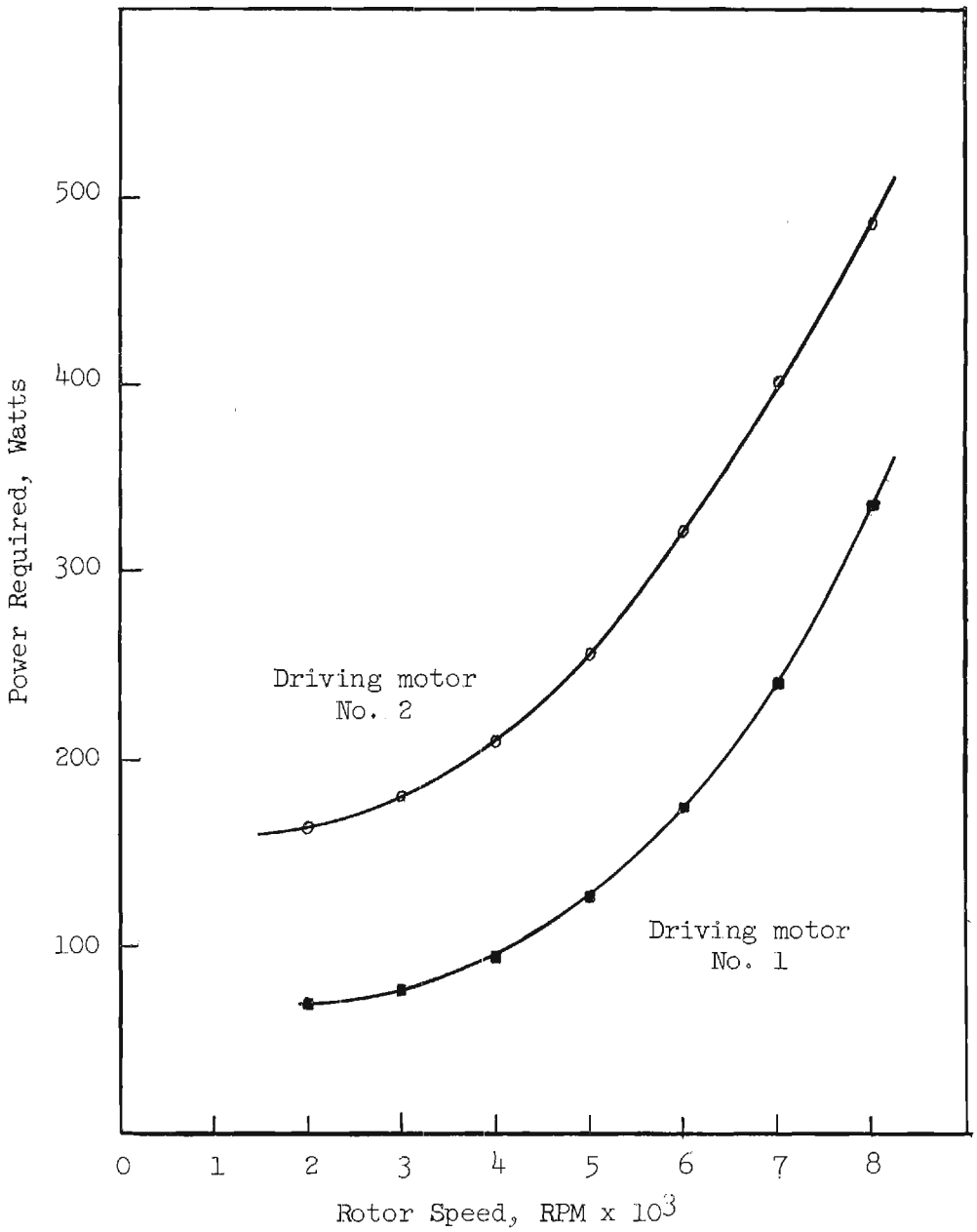

Figure 18. Power Consumption of the Centrifugal Separator.

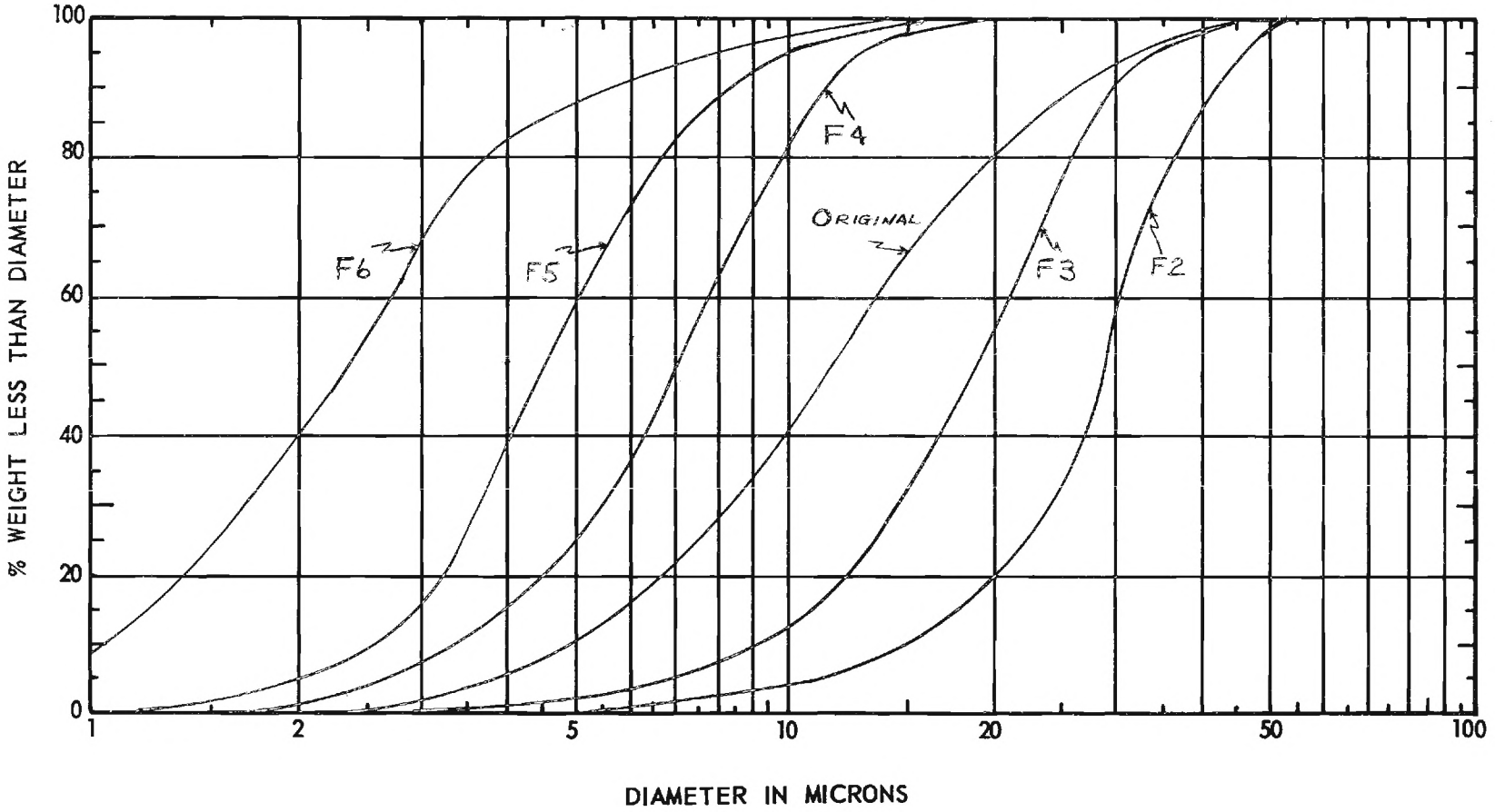

Figure 19. Size Distributions of Talc Powder Collected at Various Positions on the Centrigual Classifier Rotor.

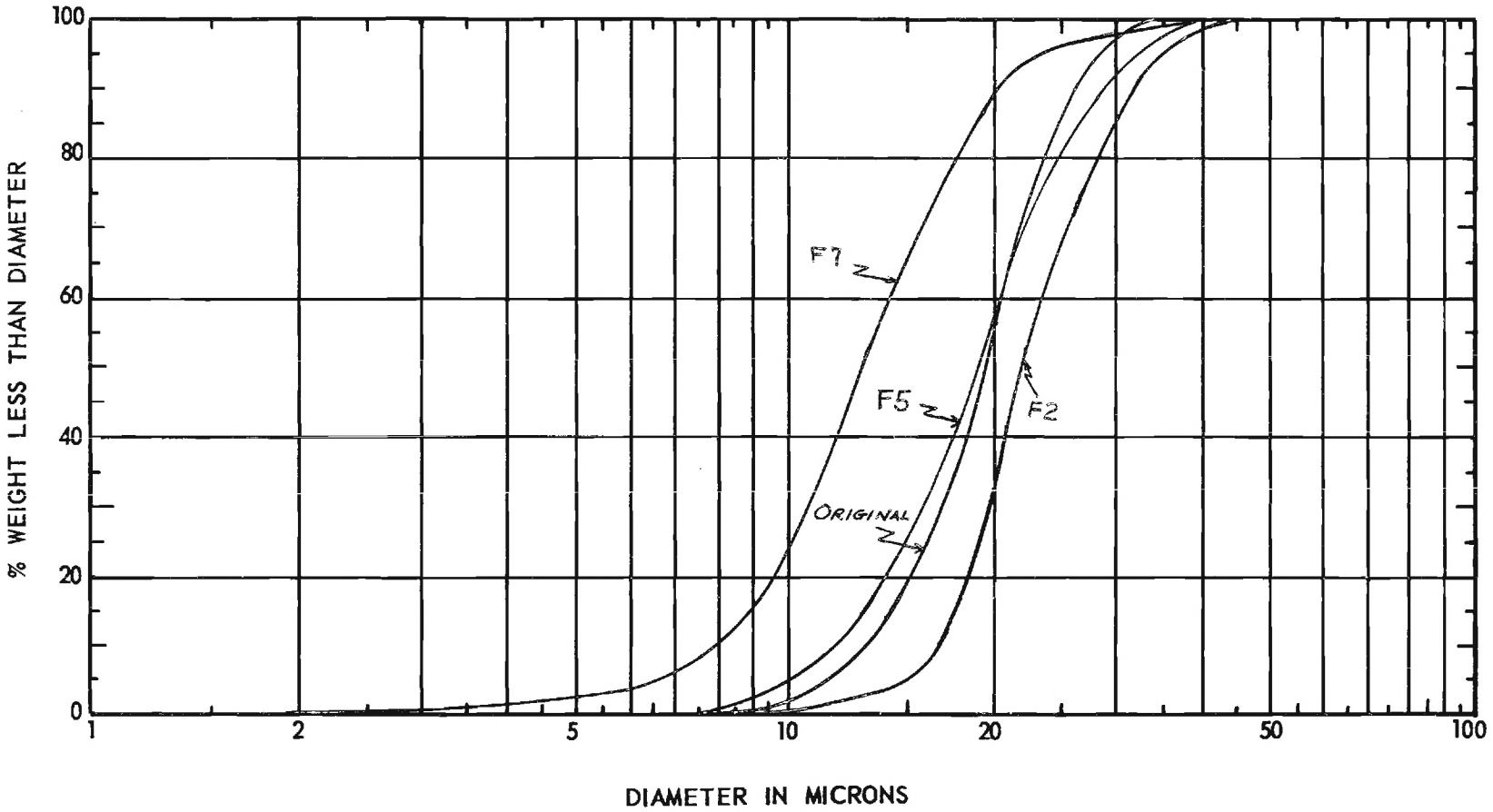

Figure 20. Size Distributions of Glass Beads Collected at Various Positions on the Centrifugal Classifier Rotor.

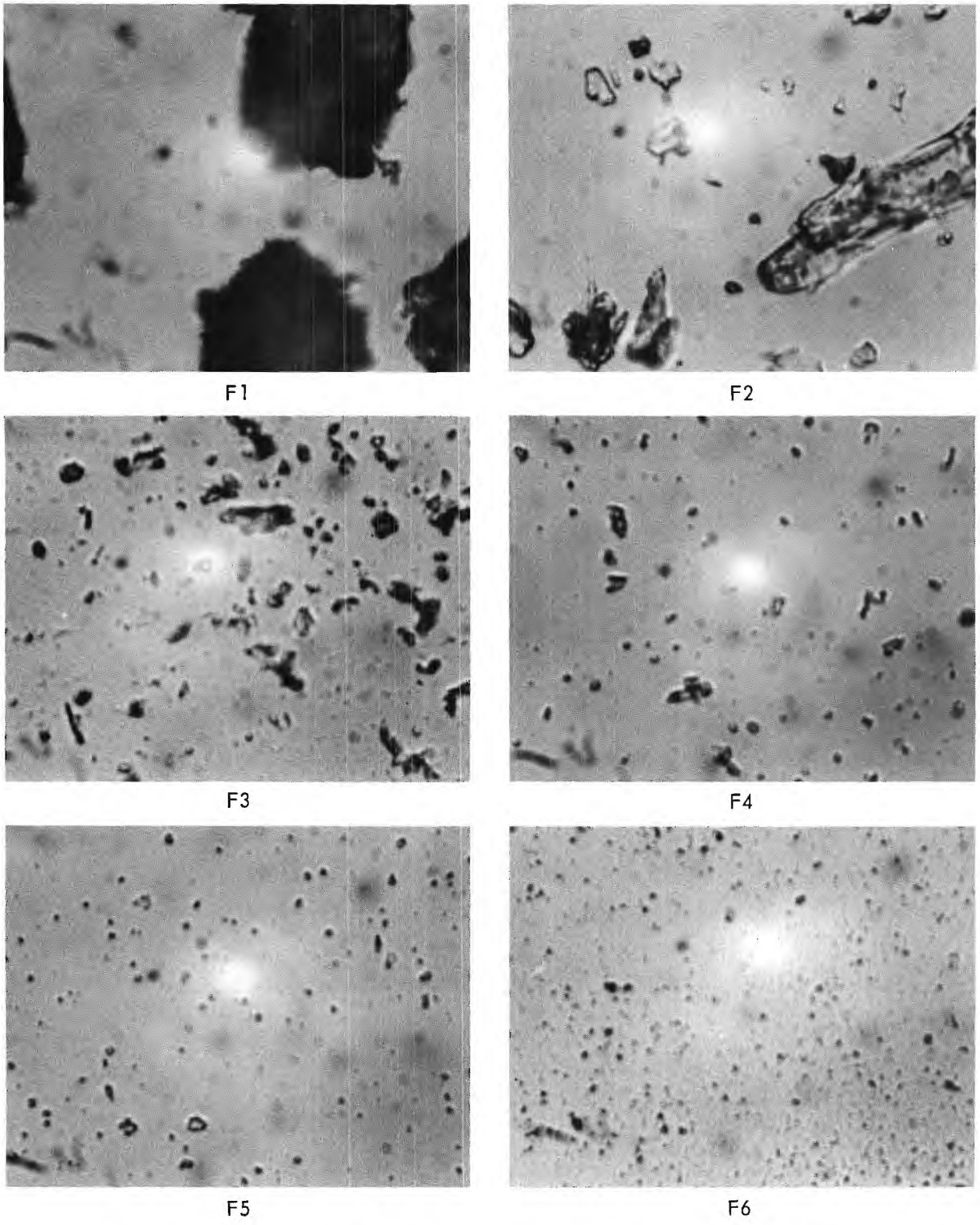

Figure 21. Micrographs of Various Size Fractions of Talc Collected on the Centrifugal Classifier Rotor (Magnification, 788X).

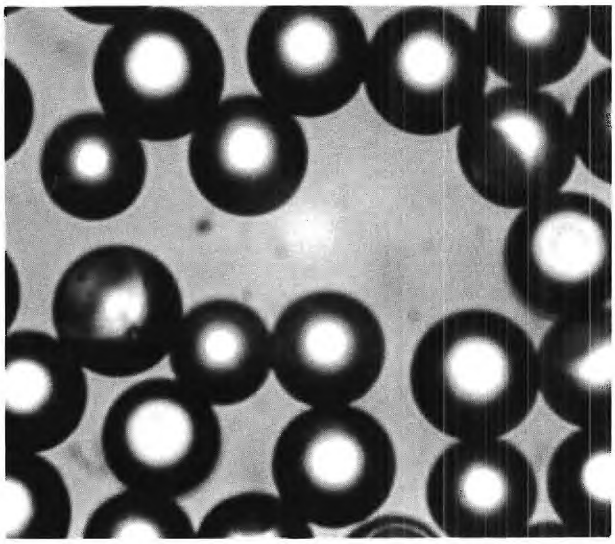

F1

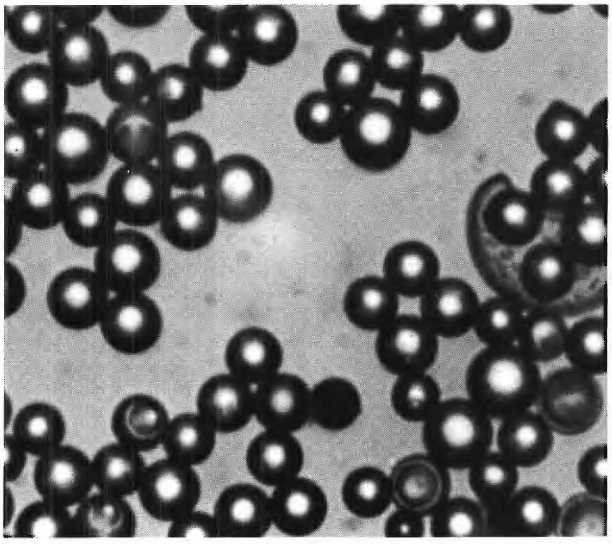

F2

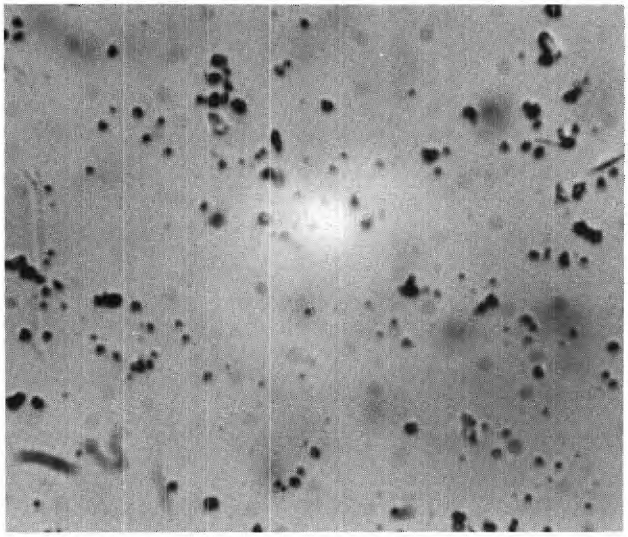

F3

Figure 22. Micrographs of Various Size Fractions of Glass Beads Collected on the Centrifugal Classifier Rotor (Magnification, 788X).

ports open. The classification of talc indicated in Figure 19 was accomplished at 6000 rpm with a secondary air flow rate of 0.25 cfm and all pressure relief ports open.

VI. DISCUSSION OF RESULTS

A. Centrifugal Separator

As is evident from the results presented in the preceding section, a highly efficient centrifugal separator has been produced that is capable of extracting particulate matter from an air stream with efficiencies approaching 100 per cent. TiO_2 aerosol which was the most difficult to collect of all dusts tested, due to its predominance of sub-micron particles, was collected under varying conditions with the efficiencies previously shown in Table VII. For this series of runs, the penetration, or material passing uncollected through the separator, showed a linear relationship with the square root of the volumetric flow rate divided by the rotor speed when plotted on a logarithmic-probability graph. This experimental result has been justified by a rather simple theory which combines the assumed particle cut diameter of the separator with a logarithmic normal distribution of particle sizes. If it is assumed that a particle in the separator moves with a velocity such that its drag forces are governed by Stokes' law then the following expression may be written

$$\frac{4\pi^2 \rho_p \delta^2 r N^2}{18\mu} = u_r \propto Q \qquad (23)$$

where ρ_p is the density of the particle, δ is the cut-size particle diameter, r is the radius of rotation, N is the rotor speed, μ is the fluid viscosity, u_r is the particle velocity, and Q is the volumetric flow rate of aerosol. Rearranging equation 23 gives

$$\delta^2 N^2 = k_1 Q \qquad (24)$$

TABLE VII

COLLECTION EFFICIENCY OF THE CENTRIFUGAL AIR CLEANER FOR TiO_2 AEROSOL

Run No.	Rotor Speed, N (RPM)	Vol. Flow Rate, Q (CFM)	Weight Material on Rotor (Gm)	Weight Material on Foil (Mg)	Penetration (100 - η) (%)	Collection Efficiency η (%)	$\frac{\sqrt{Q}}{N} \times 10^4$ $(\sqrt{CFM}/RPM)$
1	2000	0.11	0.350	6.83	1.95	98.05	1.65
2	3000	0.12	0.250	1.05	0.42	99.58	1.15
3	3000	0.24	0.577	21.48	3.60	96.40	1.63
4	4000	0.14	0.800	2.02	0.25	99.75	0.94
5	4000	0.24	0.162	1.41	0.87	99.13	1.22
6	4000	0.38	0.235	6.29	2.68	97.32	1.54
7	5000	0.17	0.803	1.27	0.16	99.84	0.82
8	5000	0.38	1.044	10.49	0.995	99.01	1.23
9	6000	0.20	1.700	0.82	0.05	99.95	0.74
10	6000	0.38	0.458	1.59	0.35	99.65	1.03
11	6000	0.49	0.910	≈ 7.53	0.83	99.17	1.16
12	7000	0.17	0.763	0.05	0.01	99.99	0.59
13	7000	0.34	0.761	0.72	0.095	99.91	0.83
14	7000	0.46	1.265	7.40	0.58	98.42	0.97
15	7000	0.52	0.650	8.20	1.25	98.75	1.03
16	8000	0.23	1.050	0.005	0.05	99.95	0.60
17	8000	0.41	1.396	0.50	0.50	99.50	0.80
18	8000	0.53	0.379	0.36	0.36	99.64	0.91

Note: Particle concentration in feeding aerosol, c ≒ 6 gm/m^3 (≒ 1/6 gm/ft^3).

or $$\delta = k_2 \frac{\sqrt{Q}}{N} \qquad (25)$$

where k_1 and k_2 are constants or proportionality. The results of Table VII are shown plotted on a logarithmic-probability grid in Figure 23. It will be noted that the linear relationship disappears above about 6000 rpm and is believed to be due to transition from laminar to turbulent conditions within the rotor.

The separator unit is capable of essentially continuous operation if the material collected within the rotor assembly is occasionally washed down by water injection.

Power consumption is greater for the present design of centrifugal separator than for comparable devices such as high efficiency filters. This condition may, in all probability, be considerably improved by redesigning the bearing system to decrease the frictional losses incurred there.

B. Centrifugal Classifier

The specially designed classifier rotor has given encouraging results for the classification by size of particulate matter. The classification attained has been shown to be strongly dependent on the type of centrifugal field present within the rotor, the pressure rise, the aerosol flow rate and the rotor speed. Excellent classification of talc has been achieved with the finest fraction having a mass mean diameter of approximately 2 microns. One limiting factor in the classification achieved to date has been the relatively ppor state of deagglomeration of materials in and around the sub-micron range. It is believed that classification may be extended into the sub-micron range by operating at reduced pressures and using particle dispersers and deagglomeration of improved design.

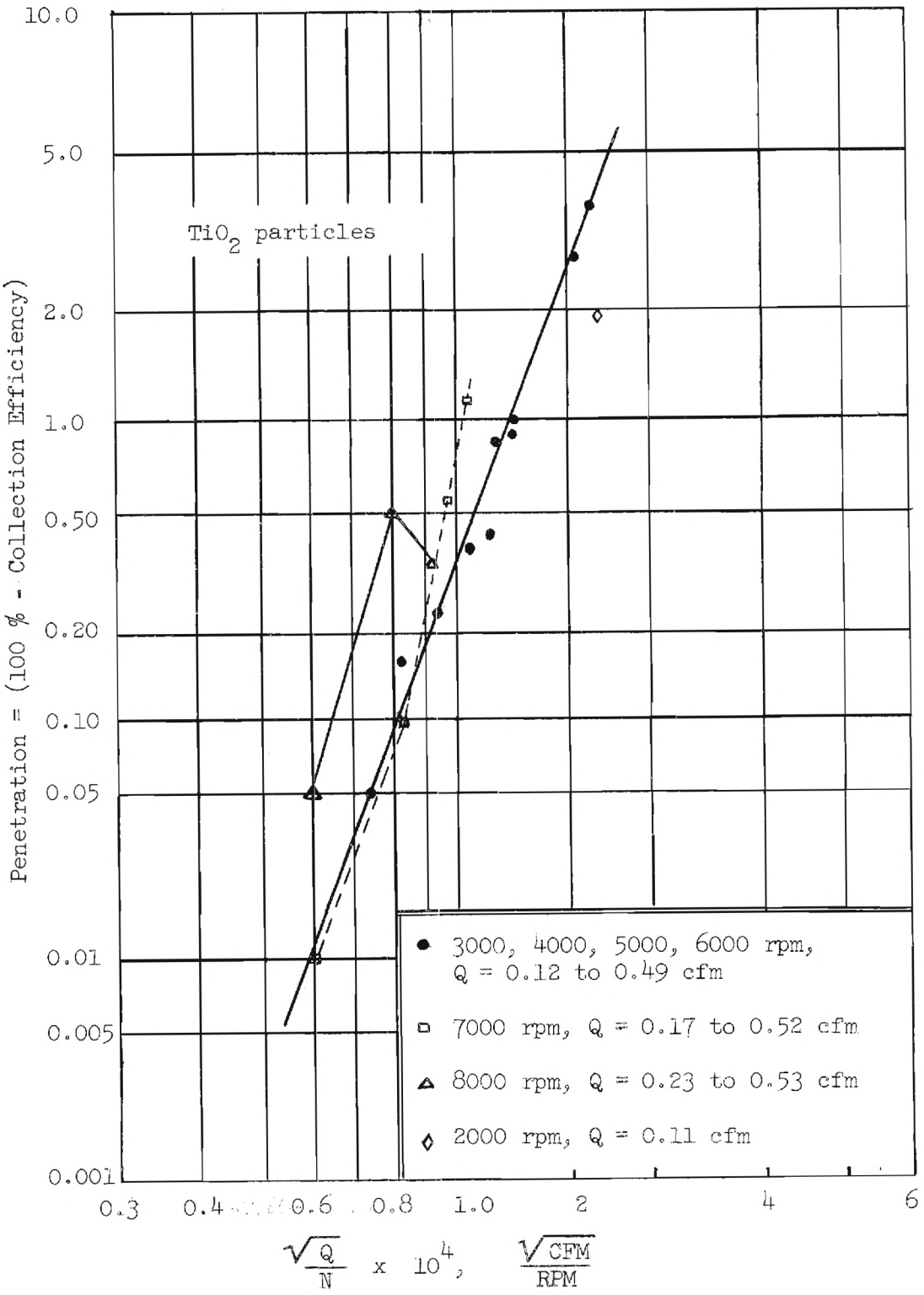

Figure 23. Collection Efficiency of the Centrifugal Separator as a Function of the Aerosol Flow Rate and the Rotor Speed.

VII. CONCLUSIONS

The following general conclusions may be stated from the results of this study:

1. A mechanical centrifugal separator is capable of extracting particulate matter from an air stream with separation efficiencies on a mass basis of essentially 100 per cent.

2. A centrifugal separator with provisions for sludge removal is capable of essentially continuous operation.

3. The collection efficiency of one centrifugal separator is a linear function of the logarithm of the square root of the flow rate divided by the rotor speed and the collection efficiency on a probability scale. This linear relationship disappears above about 6000 rpm due to, it is believed, a transition from laminar to turbulent flow.

4. A centrifugal rotary dust separator is an efficient device for the removal of particulate matter from an air stream up to unusually high dust concentrations. Such a device is believed to have promise for a variety of laboratory and industrial applications in which high separation efficiency is required over a wide range of particle sizes with essentially continuous operation.

5. A centrifugal classifier of similar design in many respects to the separator promises to permit the classification by particle size of aerosols composed of irregular and spherical particles.

6. The primary limiting factor on the extent of classification that can be achieved with a centrifugal classifier is the initial particle dispersion and deagglomeration. Other operating variables such as rotor

speed, aerosol flow rate and pressure-rise also strongly influence the classification.

7. A centrifugal separator presently requires more power for operation than more conventional devices such as filters or cyclones; however, its use may be justified in specialized applications by its excellent separation efficiency over a wide range of particle sizes, its essentially continuous operation, and its compactness.

VIII. RECOMMENDATIONS

A new design for the bearing system of the centrifugal separator should be constructed in which the rotor assembly is supported by an air bearing. This arrangement would significantly decrease the friction losses which are believed to be the major cause for the high power consumption of the present centrifugal separator. By proper design, the separator could also readily be driven by air pressure, thus further utilizing the motive power of air employed for supporting the rotor assembly. Some further studies should be conducted to determine the best type of wash-down design. The present design allows accumulation of material to occur on the housing assembly opposite the sludge discharge holes in the rotor. The peripheral pressure rise tends to hold this material on the housing assembly with a resulting build up of sludge and decrease in clearance between the rotor and housing.

The centrifugal classifier should be further tested with careful control of such variables as aerosol flow rate, pressure rise, secondary air flow and rotor speed. If possible, the type of flow field present in the classifier should be determined, i.e., it should be established whether the field is a forced vortex, free vortex, etc., and the resulting classification should be compared with that theoretically predicted from a calculation of particle trajectories in the same types of force fields.

The possibility of classification into the sub-micron region should be evaluated by operating the centrifugal separator at low pressure or in gases of extraordinary long mean free path lengths.

Respectfully submitted:

[redacted]

Clyde Orr
Project Director

Approved:

[redacted]

Frederick Bellinger, Chief
Chemical Sciences and Materials Division